

DECLARATION

DECLARATION BY THE CANDIDATE

This thesis is my original work and has not been presented to any university for purposes of an award of a degree.

Sign..... Date.....

OGANDO FELIX OCHIEN’G **SC/PGP/019/08**

DECLARATION BY SUPERVISORS

This thesis has been submitted for examination with our approval as the university supervisors.

Sign..... Date.....

PROF. K.M. KHANNA,

Department of Physics

University of Eldoret.

Sign..... Date.....

DR. K.M MUGURO,

Department of Physics

University of Eldoret.

DEDICATION

To my dear wife Beatrice Atieno, daughter Stacy Patience, son Stephen Baraka and dear parents Charles Ogando Obiero and Philister Auma Ogando.

ABSTRACT

Superconductivity nucleation phenomenon in superconductors under an applied magnetic field close to the upper critical field H_{C3} has been studied by many authors. Physicists Saint-James and De Gennes were the first to study the surface nucleation phenomenon for a semi-infinite super-conductor occupying the half space and placed in an applied magnetic field which is parallel to the surface of the superconductor. When the applied magnetic field is spatially homogeneous and close to H_{C3} , a superconducting layer or sheath nucleates on a portion of the surface at which the applied field is tangential to the surface. In the case of non-homogeneous applied magnetic fields, interior nucleation may occur first when the applied field is decreased below the upper critical field. The research is interested in the rotational velocity of a magnitude that would generate a fictitious magnetic field that exceeds H_{c1} (the upper limit of the magnetic field for type – I superconductors). The magnitude of H_{c1} is around 0.2 T. This requires that the angular velocity, ω be around 10^9 s^{-1} and it is not possible to experimentally attain such a high value for a mechanical rotation. However, such local rotations could be generated in a superconductor by high frequency ultrasound and we could study the possibility of the nucleation of a vortex by sound. A superconducting cylinder rotated at an angular velocity of ω about its symmetry axis develops a magnetic moment \mathbf{M} . It is this possibility of the nucleation of a vortex by sound that has been theoretically studied in this thesis. For a vortex to enter a superconductor, the Gibb's free energy of the system must be lowered. Calculations that showed how sound enters the problem were done and equations connecting the generated magnetic fields \mathbf{B}_s , rotating cylinder thickness d , rotational angular velocity Ω , ultrasound angular velocity ω , amplitude U_0 and wavelength λ , were derived. Calculations and analysis revealed the following major results; the rotating cylinder thickness d and the ultrasound wavelength λ are connected by the equation, $d = 0.5 \lambda$; to achieve high rotational angular velocities, Ω desired for the superconducting cylinder, its thickness d must be kept very small; the generated magnetic field and rotational angular velocity of the superconducting cylinders are connected by the equation, $\mathbf{B}_s = 6.82 \times 10^{-3} \Omega$. These results imply that it is possible to generate values of fictitious magnetic fields \mathbf{B}_s , of the order 10^3 T that exceed H_{c1} and hence nucleation of a vortex in a superconductor can be assisted by ultrasound.

TABLE OF CONTENTS

DECLARATION	i
DEDICATION	ii
ABSTRACT	iii
LIST OF TABLES	viii
LIST OF FIGURES	x
LIST OF SYMBOLS	xiii
DEFINITION OF TERMS	xvii
ACKNOWLEDGEMENT	xxvii
CHAPTER ONE	1
INTRODUCTION	1
1.1 Superconducting State	1
1.2 Flux Quantum in a Superconductor	2
1.3 Rotation of Superconducting Cylinder.	5
1.4 Statement of the Problem.....	7
1.5 Significance of the Study.....	7
1.6 Objectives	8
CHAPTER TWO	9
LITERATURE REVIEW	9
2.1 Introduction.....	9
2.2 Microscopic Theory of Superconductivity	11
2.3 Characteristics of Superconductivity.	17
2.3.1 Zero Electrical Resistance.....	18
2.3.2 Superconducting Phase Transition.....	19
2.3.3 Meissner Effect	20
2.4 Types of Superconductors.....	23
2.4.1 Type-I Superconductors.....	23

2.4.2	Type-II Superconductors.	23
2.5	Superconducting Vortices.....	26
2.6	Vortices near Lower Critical Field.	30
2.7	The Mixed State.....	31
2.8	Critical Current in the Mixed State.....	31
2.9	Role of Inhomogeneities.....	32
2.10	Nucleation of Superconducting Vortices.....	35
2.11	Nucleation of Vortices through Mechanical Rotations.....	36
	CHAPTER THREE.....	39
	METHODOLOGY.....	39
3.1	Introduction.....	39
3.2	Nucleation of Superconducting Vortices.....	39
	CHAPTER FOUR.....	46
	RESULTS AND DISCUSSION.....	46
4.1	Introduction.....	46
4.2	Ultrasound amplitude U_0 and rotating slab thickness, d	46
4.3	Rotational angular velocity, Ω of the superconducting cylinder.....	50
4.4	Relationship between angular velocities of the rotating superconducting cylinder and ultrasound.....	53
4.5	Generated magnetic field B_s in a rotating superconducting slab.....	60
	CHAPTER FIVE.....	68
	CONCLUSIONS AND RECOMMENDATIONS.....	68
5.1	Conclusions.....	68
5.2	Recommendations for Future Research.....	69
	REFERENCES.....	70

LIST OF TABLES

Table 4.1: Calculated values of ultrasound frequency f_s , thickness d of the rotating superconducting slab and ultrasound amplitude U_o using assumed values of ultrasound wavelength, λ_s	48
Table 4.2: Calculated values of angular velocity Ω of a rotating superconducting slab of different values of thickness, d and ultrasound angular velocity, ω_s (as calculated from table 4.1) for constant ultrasound amplitude, $U_o = 0.23\text{nm}$	51
Table 4.3: Calculated values of angular velocity Ω of a rotating superconducting slab of thickness $d = 0.25 \times 10^{-6}$ m with ultrasound of amplitude, $U_o = 0.23 \times 10^{-9}$ m and varying angular frequency, ω_s	53
Table 4.4: Calculated values of angular velocity Ω of a rotating superconducting slab of thickness $d = 0.75 \times 10^{-6}$ m with ultrasound of amplitude, $U_o = 0.23 \times 10^{-9}$ m and varying angular velocities, ω_s	55
Table 4.5: Calculated values of angular velocity Ω of a rotating superconducting slab of thickness $d = 1.75 \times 10^{-6}$ m with ultrasound of amplitude, $U_o = 0.23 \times 10^{-9}$ m and varying angular velocities, ω_s	57
Table 4.6: Calculated values of generated magnetic field B_s , for different values of ultrasound angular velocity ω , and rotational angular velocity Ω of the superconducting slab of varying slab thickness, d . The ultrasound amplitude is constant, $U_o = 0.15$ nm.....	60

Table 4.7: Calculated values of generated magnetic field B_s , for different values of ultrasound angular velocity ω , and angular velocity Ω of rotation of the superconducting slab of varying slab thickness, d . The ultrasound amplitude is constant, $U_o = 0.23$ nm..... 62

Table 4.8: Calculated values of generated magnetic field B_s , for different values of ultrasound angular velocity ω , and rotational angular velocity Ω of the superconducting slab of varying slab thickness, d . The ultrasound amplitude is constant, $U_o = 0.40$ nm..... 64

LIST OF FIGURES

Figure 2.1: Graph of resistance versus temperature for both conductors and superconductors. T_c is the critical transition temperature.....	10
Figure 2.2: Behaviour of heat capacity (C) and resistivity (ρ) at the superconducting phase transition.....	20
Figure 2.3: The Meissner effect or the expulsion of a magnetic field from a superconductor as it transitions to its superconducting state.....	22
Figure 2.4: Variation of internal magnetic field (B) with temperature (T) for type I and type II superconductors.....	24
Figure 2.5: The variation of internal magnetic field (B) with applied external magnetic field (H) for type-I and type-II superconductors.....	25
Figure 2.6: Superconducting vortices (white spots) as imaged by the magnetic decoration technique.....	28
Figure 2.7: Illustrates that magnetic field lines (black) can only penetrate a superconductor through a vortex.....	28
Figure 2.8: The possible form of the velocity of a vortex \mathbf{v} as a function of the local current density, \mathbf{j}	34
Figure 4.1: The linear relationship between the thicknesses d , of a rotating slab and the wavelength λ , of the ultrasound with constant amplitude of 0.23 nm.....	49

- Figure 4.2: Relationship between the angular velocity Ω and the thickness d of a rotating slab of a superconducting cylinder. The ultrasound amplitude is constant, $U_o = 2.3 \times 10^{-10}$ m..... 52
- Figure 4.3: Relationship between the rotational angular velocity, Ω of the superconducting slab and the ultrasound angular velocity, ω . The slab thickness, $d = 0.25\mu\text{m}$ and ultrasound amplitude, $U_o = 0.23 \times 10^{-9}$ m..... 54
- Figure 4.4: Relationship between the rotational angular velocity, Ω of the superconducting slab and the ultrasound angular velocity, ω . The slab thickness, $d = 0.75\mu\text{m}$ and ultrasound amplitude, $U_o = 0.23 \times 10^{-9}$ m..... 57
- Figure 4.5: Relationship between the rotational angular velocity, Ω of the superconducting slab and the ultrasound angular velocity, ω . The slab thickness, $d = 1.75\mu\text{m}$ and ultrasound amplitude, $U_o = 0.23 \times 10^{-9}$ m..... 58
- Figure 4.6: Relationship between the rotating superconducting slab thickness d , the angular velocity ω , of the ultrasound (of constant ultrasound amplitude of $U_o = 0.23$ nm.) and the angular velocity, Ω of rotation of the superconducting cylinder..... 59
- Figure 4.7: Indicates a positive linear relationship between the angular velocity, Ω of the rotating superconducting slab and the generated magnetic field, \mathbf{B}_s , when the ultrasound amplitude is 0.15nm..... 61

- Figure 4.8: Indicates a positive linear relationship between the angular velocity, Ω of the rotating superconducting slab and the generated magnetic field, \mathbf{B}_s when the ultrasound amplitude is 0.23nm..... 63
- Figure 4.9: Indicates a positive linear relationship between the angular velocity, Ω of the rotating superconducting slab and the generated magnetic field, \mathbf{B}_s when the ultrasound amplitude is 0.40nm..... 65
- Figure 4.10: Relationship between the generated magnetic field \mathbf{B} , and the slab thickness d , of the superconducting cylinder for different values of ultrasound amplitude, $U_o = 0.15, 0.23$ and 0.40 nm..... 66

LIST OF SYMBOLS

A:	Magnetic vector potential
B:	Magnetic field intensity.
c:	Speed of light in a vacuum = $3.00 \times 10^8 \text{ ms}^{-1}$
C:	Heat Capacity
e:	Electron charge = 1.60×10^{-19} Coulombs
E:	Applied electric field.
E_F:	Fermi Energy
E (p):	Fermi surface in p -space
F_L:	Lorentz Driving Force
F_P:	Elementary pinning force
G:	Gibbs free energy, $G = H - TS$
h:	Plancks Constant = $6.63 \times 10^{-34} \text{ m}^2 \text{ kg} / \text{ s}$
H:	Enthalpy
H:	Magnetic Field
H_c:	Critical Magnetic field of a superconductor
H_{c1}:	Lower critical field
H_{c2}:	Upper critical field

H_{sh}	Superheating field
⟨H_{in}⟩:	Average internal field
I_c:	Critical Current
J:	Current density
J_{nulc}	Nucleation Current Density
J_{pin}	Depinning Current
k:	Ginsburg – Landau parameter, $k = \lambda/\xi$
K:	Kelvin
m:	Mass of an electron = 9.11×10^{-31} kilograms
M:	Magnetization; Magnetic Moment
m*:	Electron effective mass
N_A:	Number of vortices per unit area
N_b	Niobium
P:	Momentum
P_F:	Fermi Momentum
Q:	Gauge Invariant vector potential
R_H:	Hall co-efficient

$S:$	Entropy
$T:$	Temperature
$T_c:$	Critical Temperature of a superconductor
$\mathbf{u}(\mathbf{r}, t):$	Displacement vector field
$\dot{\mathbf{u}}:$	Velocity of ions
$\mathbf{V}:$	Velocity of the Cooper pairs
$V_F:$	Fermi Velocity
$\omega:$	Angular velocity
$\rho:$	Charge density; also resistivity.
$\xi:$	Coherence length
$\Psi:$	Complex order parameter
$\Omega_D:$	Debye Frequency
$\sigma:$	Electrical Conductivity
$\epsilon:$	Electron energy of superconductors
$\Delta:$	Energy gap: Separates excited state of the electron system from the ground state.
$\gamma:$	Gyroscopic Ratio
$\chi:$	Magnetic susceptibility Cooper pairs.

λ :	Penetration depth.
ϕ :	Phase of the superfluid
\hbar :	Reduced Plancks Constant given by $\frac{h}{2\pi}$
δ_r :	Spatial spread of the Cooper pairs of electrons
ϕ_0	Elementary Flux Quantum

DEFINITION OF TERMS

Absolute Zero Temperature: The lowest possible temperature, at which point the atoms of a substance transmit no thermal energy - they are completely at rest. It is 0 degrees on the Kelvin scale, which translates to -273.15 degrees Celsius (or -459.67 degrees Fahrenheit).

Acoustic Waves: Sound waves.

Adiabatic Systems: A system that does not exchange any heat with its environment.

Angular Momentum, L : The quantity of rotation of a body, which is the product of its moment of inertia and its angular velocity. $L = \mathbf{r} \times \mathbf{mv}$

Angular Velocity ω : The rate of change of angular position (displacement) of a rotating body. $\omega = \frac{d\phi}{dt}$

BCS: Superconductivity theory developed by J. Bardeen, L.N Cooper and J.R. Schrieffer in 1957.

Binding Energy: The energy that holds a nucleus together.

Bound State: A composite of two or more building blocks (particles or bodies) that behaves as a single object.

Ceramic – A product made from clay or related material.

Ceramic Compounds – These are compounds that contain planes of copper and oxygen atoms. **Coherence Length, ξ :** Distance over which Ginsburg – Landau order parameter

$\phi(r)$ can change without an appreciable change in energy. It's also the radius of core of a vortex.

Conductor: Material of low resistivity i.e. conducts electricity well.

Conventional Superconductivity – This is superconductivity that is exhibited by metallic alloys and doped semiconductors.

Cooper Pairs: Paired electrons that constitute the charge carrier of supercurrent. Electron pairs as a result of the weak interaction between them.

Critical Current: Value of current above which superconductivity disappears. It is the highest current that can flow through a particular superconducting wire or tape.

Critical Magnetic Field B_c : Highest field sustained by a Type – I superconductor. Type II superconductors have lower B_{c1} and upper B_{c2} critical fields with thermodynamic critical field. $B_c = (B_{c1}B_{c2} \ln k)^{1/2}$

Critical Temperature, T_c : Temperature below which superconductivity occurs. It is the transition temperature.

Crystal Lattice: The symmetrical three-dimensional arrangement of atoms inside a crystal.

Cuprates: These are high temperature superconductors.

Current Density, J : Electric current per unit cross sectional area, A/m^2 .

Debye Frequency, Ω_D : A theoretical maximum frequency of vibration for the atoms that make up the crystal.

Depinning: Release of vortices from being pinned.

Diamagnetism: Phenomenon exhibited by materials like copper or bismuth that become magnetized in a magnetic field with a polarity opposite to the magnetic force. Unlike iron, they are slightly repelled by a magnet. It is the property of being repelled by both poles of a magnet.

Dielectric Materials: A non-conducting material with equal number of positive and negative charges. Charges get polarized under applied electric field.

Doped Semiconductors: Semiconductors in which a small amount of one atom has been added to replace another, as in the superconductor $(\text{La}_{0.9}\text{Sr}_{0.1})_2\text{CuO}_4$

Electrical Conductivity: Ratio $\sigma = J/E$ of the current density J to the applied electric field that causes it to flow.

Electromagnetic Radiation: A kind of radiation including visible light, radio waves, gamma rays and X-rays, in which electric and magnetic fields vary simultaneously. **It** is self sustaining energy with electric and magnetic field components. They are transverse waves.

Electron Effective Mass, m^* : Experimentally measured mass, m^* , that deviates from actual mass, m_e .

Electron – Phonon Interaction: Cooper pair coupling mechanism in superconductors.

Energy Band: Set of very closely spaced energy levels.

Energy Gap, Δ : Separation in energy between two energy levels.

Energy Spectrum: An arrangement of particle energies (as of alpha particles or photoelectrons) in a heterogeneous beam that is analogous to the arrangement of frequencies in an optical spectrum.

Enthalpy, H: Measure of the total energy of a thermodynamic system. It includes the internal energy, which is the energy required to create a system, and the amount of energy required to make room for it by displacing its environment and establishing its volume and pressure.

Entropy, S: Measure of the number of specific ways in which a system may be arranged, often taken to be a measure of disorder. The entropy of an isolated system never decreases, because isolated systems spontaneously evolve towards thermodynamic equilibrium, which is the state of maximum entropy.

Fermi – Energy: Energy of highest occupied level in k-space for fermions.

Fermi – Surface: Energy surface bounding occupied region of k-space for fermions.

Ferromagnetic Materials: Electronic spins polarized in the same direction resulting in high magnetic field.

FLL: Flux Line Lattice.

Flux, Φ : Quantity of magnetic field, $\Phi = \mathbf{B} \cdot \mathbf{A}$, with unit weber = Tm^2 .

Flux Flow: Faster motion of magnetic flux when vortex pinning forces are weak and dominated by the Lorentz force.

Flux Line: Another name for vortex.

Fluxoid: A quantity of magnetic flux, Φ , in a vortex with the quantum value $\Phi_0 = h/2e$.

Flux Quantum: $\Phi_0 = h/2e$, amount of magnetic flux in a vortex.

Gap: Separation energy, especially that between normal and superconducting states.

Gibbs Free Energy: $G = H - TS$.

Gyromagnetic Effect: An effect that arises from the relation between the angular momentum and the magnetization of a magnetic substance.

Gyroscopic Ratio, γ : The ratio of a particle's or a system's magnetic dipole moment to its angular momentum. For the orbital motion of an electron, $\gamma = e/2mc$.

Hall Effect: Establishment of transverse electric field in current carrying conductor located in a transverse magnetic field.

Hard Superconductor: A superconductor with pinning forces strong enough to prevent flux motion.

Heat Capacity: The heat required to raise the temperature of a substance by unit temperature interval under specified conditions, usually measured in joules per Kelvin.

High Temperature Superconductors: Materials that behave as superconductors at unusually high temperatures. The first high- T_c superconductor was discovered in 1986 by IBM researchers Karl Müller and Johannes Bednorz.

Intermediate State: A state of Type I superconductivity involving mixture of normal and superconducting regions arising because of non-zero demagnetization factor.

Isotope Effect: Role of lattice vibrations in the electron-phonon interaction responsible for the onset of superconductivity.

Latent Heat: The quantity of heat absorbed or released by a substance undergoing a change of state, such as ice changing to water or water to steam, at constant temperature and pressure. Also called heat of transformation.

Lattice: A regular, periodic configuration of points, particles, or objects throughout an area or a space, especially the arrangement of ions or molecules in a crystalline solid.

Lenz's Law: The induced current and the accompanying magnetic flux are in directions that oppose the change in flux through a circuit.

Lorentz Driving Force, F_L : $F_L = I \times B = J \times \Phi$, actually a force per unit length.

Magnetic Field, H : Magnetic flux per unit area held perpendicular to H .

Magnetic Moment: Magnetic analogue of electric dipole moment.

Magnetization, M : Magnetic dipole moment per unit volume.

Meissner Effect: Expulsion of the field from the interior of a superconductor when it's placed in a weak magnetic field.

Mixed state: Type II superconductor state of partial flux exclusion existing in the applied field range $B_{c1} < B_{app} < B_{c2}$.

Momentum: A quantity expressing the motion of a body or system equal to the product of the mass of a body and its velocity and for a system equal to the vector sum of the products of mass and velocity of each particle in the system.

MRI Machines: Magnetic Resonance Imaging machines

Normal State: Synonymous with non – superconducting state.

Ohm's Law: $V = IR$, or in normalized form, $\mathbf{E} = \mathbf{J}\rho$

Pauli Principle: States that no two electrons can have the identical quantum mechanical state in the same atom. No pair of electrons in an atom can have the same quantum numbers n , l , m_l and m_s . The assertion that no two fermions can have the same quantum number.

Penetration Depth, λ : Distance externally applied magnetic field \mathbf{B}_{app} reaches inside a superconductor.

Permittivity: The ability of a substance to store electrical energy in an electric field.

Perturbation Theory: Comprises mathematical methods that are used to find an approximate solution to a problem which cannot be solved exactly, by starting from the exact solution of a related problem. Perturbation theory is applicable if the problem at hand can be formulated by adding a "small" term to the mathematical description of the exactly solvable problem.

Phonons – Packets of sound waves that are present in the lattice as it vibrates.

Pinning: Holding in place or refraining the motion of a vortex.

Polycrystalline Materials: Materials that are composed of many crystallites of varying size and orientation. The variation in direction can be random (called random texture) or

directed, possibly due to growth and processing conditions. Fiber texture is an example of the latter.

Resistance, R: Measure of heat dissipation of wire carrying electric current; $R = \rho L/A$ for wire of resistivity ρ , length L and cross-section area A .

Resistivity ρ : Property of a metal that measures its ability to carry an electric current

Semiconductor: A material with electrical conductivity between those of a metal and an insulator.

Soft Superconductor: One in which the pinning forces are not strong enough to prevent flux motion.

Specific Heat: Quantity of heat energy that must be added to a material to make its temperature rise by 1°C .

Spin: An intrinsic form of angular momentum carried by elementary particles, composite particles (hadrons) and atomic nuclei.

Standing Wave: A vibration of a system in which some particular points remain fixed while others between them vibrate with the maximum amplitude.

Strain: A measure of how much an object is being stretched

Superconductivity: Vanishing of electrical resistance of a conductor at very low temperatures.

Supercurrent: A superconducting current, that is, electric current which flows without dissipation.

Super fluidity: Flow of a liquid such as Helium below lambda point (2.17 K) without viscous drag and without dissipation of heat.

Susceptibility χ : M/H - Magnetization per unit H- field in a material.

Thermal Conductivity: Coefficient measuring efficiency of thermal current flow; thermal analogue of electrical conductivity.

Thermodynamic Equilibrium: A system is in thermodynamic equilibrium when it is in thermal equilibrium, mechanical equilibrium, radiative equilibrium and chemical equilibrium. Equilibrium means a state of balance. In a state of thermodynamic equilibrium, there are no net flows of matter or of energy, no phase changes and no unbalanced potentials (or driving forces) within the system. A system that is in thermodynamic equilibrium experiences no changes when it is isolated from its surroundings.

Transverse Wave: A wave, such as an electromagnetic wave, that is propagated in a direction perpendicular to the direction of displacement of the transmitting field or medium.

Type I Superconductors: Superconductors in which superconductivity is abruptly destroyed when the strength of the applied field rises above a critical value H_c .

Type II Superconductors: Totally expels and excludes magnetic flux below lower magnetic critical field H_{c1} and upper critical field H_{c2} .

Unconventional Superconductors: These exhibit superconductivity but their physical properties contradict the theory of conventional superconductors.

Ultrasound: Sound or other vibrations having an ultrasonic frequency $> 20,000$ cps, particularly as used in medical imaging.

Viscous Drag: Resistance to flow in a liquid.

Vortex – Cylinder or tube of magnetic flux containing one quantum of flux Φ_0 ; found in type – II superconductor located in magnetic field B_{app} .

Vortex Lattice: Regular arrangement of vortices, usually in a hexagonal pattern, sometimes called Abrikosov pattern.

Wave Amplitude: The magnitude of the maximum displacement of a wave from a mean value or position.

Wave Frequency: The total number of complete oscillations or cycles in a second.

Wave Function: A function that satisfies a wave equation and describes the properties of a wave.

Wavelength: The distance between successive crests of a wave, especially points in a sound wave or electromagnetic wave.

Wigner Molecule: A **Wigner crystal** is the solid (crystalline) phase of electrons first predicted by Eugene Wigner in 1934. A gas of electrons moving in 2D or 3D in a uniform, inert, neutralizing background will crystallize and form a lattice if the electron density is less than a critical value. This is because the potential energy dominates the kinetic energy at low densities, so the detailed spatial arrangement of the electrons becomes important.

ACKNOWLEDGEMENT

It is with great pleasure that I want to thank the individuals and organizations that played a pivotal role in helping me come up with this thesis. First and foremost, my sincere appreciation goes to my supervisors Prof. K. M. Khanna and Dr. K. M. Muguro for their professional guidance and vigorous work that they put me through during the research work. Their invaluable wealth of knowledge and experience in this field really assisted me in fine tuning the thesis.

Many thanks go to the entire staff of the Physics Department, University of Eldoret, for all the assistance they extended to me whenever I needed it. I would also wish to thank Mr. Rajula Julius (Students' Affairs) and Ms. Gladys Odhacha (Deputy Vice-Chancellor's Office), both staff of University of Eldoret, for their unwavering support in piecing up the thesis.

I also have to very sincerely thank my M.Sc colleagues for all the discussions that we had together. Mr. Okuna Calvince for his moral support, positive criticisms and advices, Mr. Odoyo Maurice for supporting me with reference materials and Mr. Willice Obonyo for the journals and books he constantly sent me from South Africa.

I acknowledge my father Mr. Charles Ogando Obiero, mothers Mrs. Philister Auma Ogando and Clarice Ogando and siblings (George, Ben, Caroline, Evans, Kevin, Beryl and Victor) for their constant encouragement and support. My heartfelt gratitude is extended to my dear wife, Beatrice Atieno, who was particularly a source of motivation and encouragement.

I also wish to thank Mr. Okwara Kevin and his wife Mrs. Jane Ndubi (Directors of Alphax College – Eldoret) for allowing me sufficient time to study and carry out my research when it was apparently difficult to balance my time as their employee and student. May God richly reward you all.

Finally I thank my God for His sufficient grace, provision and strength that has continued to propel me up the academic ladder

CHAPTER ONE

INTRODUCTION

1.1 Superconducting State

The superconducting state occurs due to the presence of 0.01% of what is called ‘abnormal electrons’ while the other 99.99% free (conduction) electrons remain absolutely normal. The correlated behaviour of the small fraction of these ‘abnormal’ electrons overwhelms the rest. Due to the presence of these ‘abnormal’ electrons, the metal is a superconductor in which currents of the order of 10^5 A flow easily and the metal loses its resistance. It appears as if the normal conduction electrons do not exist at all. Only the transport properties of the electrons in a metal are affected, whereas the crystal structure of a metal is almost unchanged below the critical temperature, i.e., when a metal is in a superconducting state [1].

The superconducting state is a macro state, or it can be said to be a quantum state occurring on a macroscopic state. In a sense, the superconducting state is a ‘bridge’ between the microworld and macroworld. The ‘bridge’ allows us to study the physics of the microworld directly. Like other states of matter, superconductivity is not a property of isolated atoms, but a collective effect determined by the structure of the whole sample. Although the superconducting state is driven only by a small fraction (10^{-4} or 0.01%) of all the conduction electrons (called the ‘abnormal’ electrons), it is a many-body phenomena involving the structure of the whole sample [1].

Electrons are fermions with a spin of $\frac{1}{2}$, and obey the Fermi-Dirac statistics. In a superconductor, two electrons can form a pair which is a boson with zero spin ($\uparrow\downarrow$), or a

spin equal to 1 ($\uparrow\uparrow$). These electrons conform to the Fermi - Dirac statistics and being in a phase, can move in a crystal without friction [1].

A critical suggestion was made by Frohlich in 1950 that lattice vibrations play an important role in the interaction responsible for the onset of superconductivity. This leads to the concept of electron-phonon interaction and isotope effect. The study of different isotopes of mercury (Hg) established a relationship between the critical temperature of superconducting transition temperature, T_c and the isotope mass M [2]:

$$T_c M^{1/2} = \text{constant.} \quad 1.1$$

In 1956, Leon Cooper [3] showed that in the presence of the very weak electron-phonon (lattice) interaction, two conducting electrons are capable of forming a stable paired state. The paired state is now referred to as the Cooper pair. The size of the Cooper pair is about 10^{-4} cm which is very large compared to the distance between the two electrons which is about 10^{-8} cm. The weak electron-phonon interaction is an attractive potential between the two electrons that interact via the virtual exchange of a phonon. This concept led to the formulation of the so called Bardeen-Cooper-Shrieffer (BCS) Theory of superconductivity in 1957 [3].

1.2 Flux Quantum in a Superconductor

The elementary flux quantum in a superconductor is given by;

$$\Phi_0 = \frac{hc}{4\pi e} = 2 \times 10^{-7} \text{ Gcm}^2. \quad 1.2$$

The quantized entities that carry this magnetic flux into a type – II superconductor go by many names: Vortices, flux lines, fluxons and fluxoids. The centre of a vortex is where

the local magnetic field reaches its peak value. The magnetic field distribution is maintained by a local vortex like distribution of supercurrent and this current reaches its peak value at a distance of about ξ from the vortex axis. The region within about ξ from the vortex axis is referred to as the vortex core. The superconducting order parameter is strongly suppressed in the vicinity of the core and is zero on the vortex axis [4].

A flux vortex [4] comprises of a normal core of radius ξ (ξ is the coherence length defined as the length over which any perturbation in the superconducting order is smoothed out) carrying a quantum of magnetic flux $\Phi_0 = 2 \times 10^{-7} \text{ Gcm}^2$ surrounded by vortices of supercurrent spread over a distance λ (λ measures the exponential field penetration which is essentially the distance over which the shielding super currents flow. It is also called the penetration depth of the supercurrent). At H_{c1} , the first flux vortex is nucleated and with increasing field, their equilibrium separation is reduced such that at H_{c2} , the normal cores begin to overlap and thus the bulk of the material turns non-superconducting [4].

Commercially, the most attractive property of a type – II superconductor is its large upper critical field, H_{c2} , and it is this property which invites its use for making superconducting electromagnets that produce lossless high magnetic fields. However, for this kind of application, a superconducting wire must have large H_{c2} and must also possess the ability to carry an appreciably high transport current without resistance in a high transverse magnetic field. The resistance-less transport current in a homogenous type – II superconductor is limited to that value which just produces the field H_{c1} at its surface, as given by Silsbees' rule [4];

$$H_c = \frac{2I_c}{a} \quad 1.3$$

where I_c is the current and a is the radius of the wire.

Above H_{c1} , the sample contains both the transport current and magnetic vortex lines threading through bulk of the sample. Their co-existence results in what is known as the Lorentz driving force, F_L , acting on flux vortices,

$$F_L = \frac{1}{c} (\mathbf{B} \times \mathbf{J}) \quad 1.4$$

where \mathbf{J} is the current density and \mathbf{B} is the average magnetic induction.

This force is maximum when the transport current density \mathbf{J} is transverse to the magnetic field H and it acts on flux vortices, tending them to move. The situation with longitudinal magnetic field is more complicated [4].

Flux vortices take up helical configuration and in doing so reduce F_L . This ‘force free’ configuration results in much higher J_c values than in the transverse field case. In a homogenous wire, there is no counteracting force preventing this and an unstable situation therefore results in which the flux vortices are driven into motion. Such a motion is a dissipative process that gives rise to resistance and when this occurs, the wire ceases to be of practical interest. Clearly, to carry a large current without resistance, the flux vortices must be pinned so that their motion is inhibited. Various kinds of inhomogeneities, such as lattice defects, second phase and composition fluctuations in the material can interact with flux lines and produce pinning forces which counteract the Lorentz driving force and promote a non-equilibrium vortex distribution. The mixed state can now carry lossless transport current upto a maximum or critical value which

corresponds to the driving force being just equal to the pinning force. As inhomogeneities are progressively added, the critical current increases and the magnetization curve becomes more and more hysteretic, the two effects being closely related [4].

In real materials, inhomogeneities offer pinning forces, counteracting the driving force, and a static non-uniform vortex distribution becomes possible, provided $F_L < F_P$, where F_P is the maximum pinning force per unit volume such that;

$$F_P = -\frac{B}{4\pi} \frac{dB}{dx} \quad 1.5$$

Critical current is defined by the force balance equation;

$$F_L = F_P \quad 1.6$$

Equation 1.6 defines the critical state where the field gradient is maximum or critical and it corresponds to critical current.

1.3 Rotation of Superconducting Cylinder.

A superconducting cylinder rotated [5] at an angular velocity of ω about its symmetry axis develops a magnetic moment, \mathbf{M} .

$$\mathbf{M} = -\left(\frac{mc}{2\pi e}\right) \omega \quad 1.7$$

where m is the mass of the electron, e is the charge on the electron and c is the speed of light.

This effect is a consequence of a more general gyromagnetic effect predicted by Barnett [6]. In fact, the Barnett effect is a consequence of the Larmor Theorem. In the rotating

frame of reference, the action of the rotation on charged particles is equivalent to the action of the magnetic field;

$$H_{\omega} = \frac{\omega}{\gamma} \quad 1.8$$

where γ is the gyroscopic ratio.

For the orbital motion of the electron,

$$\gamma = \frac{e}{2mc} \approx 0.9 \times 10^7 \text{ G}^{-1}\text{S}^{-1}. \quad 1.9$$

Due to the Meissner effect [7], a magnetic field inside the cylinder would be expelled by the superconducting current induced at the surface. Thus for the total magnetic field \mathbf{B} , inside the bulk of the cylinder, one can write;

$$\mathbf{B} = \mathbf{H}_{\omega} + 4\pi\mathbf{M} \text{ and } \mathbf{B} = \mathbf{0} \quad 1.10$$

This gives London's magnetic moment;

$$\mathbf{M} = -\frac{\mathbf{H}_{\omega}}{4\pi}, \text{ or } \mathbf{M} = -\left(\frac{mc}{2\pi e}\right)\omega. \quad 1.11$$

Due to the symmetry of the problem, it is the same in the rotating and laboratory frames of reference. In this study, we are interested in the rotational velocity of a magnitude that would generate fictitious magnetic field that exceeds H_{c1} , where H_{c1} is the upper limit of the magnetic field for type – I superconductors. The magnitude of H_{c1} [4] could be around 0.2 T or 2K oe. This will require that the angular velocity ω be around 10^9 s^{-1} and it is not possible to experimentally attain such a high value for a mechanical rotation. However, such local rotations could be generated in a superconductor by high frequency ultrasound and we could study the possibility of the nucleation of a vortex by sound. It is this

possibility of the nucleation of a vortex by sound [5] that has been theoretically studied in this thesis.

1.4 Statement of the Problem

In this thesis, we are interested in the rotational velocity of a magnitude that would generate fictitious magnetic field that exceeds H_{cl} , where H_{cl} is the upper limit of the magnetic field for type – I superconductors. The magnitude of H_{cl} could be around 0.2 T or 2K oe. This will require that the angular velocity ω be around 10^9 s^{-1} and it is not possible to experimentally attain such a high value for a mechanical rotation. However, such local rotations could be generated in a superconductor by high frequency ultrasound and we could study the possibility of the nucleation of a vortex by sound.

1.5 Significance of the Study

In this study, we examine nucleation of vortices in a superconductor below the first critical field, H_{cl} and how this can be assisted by transverse sound in the gigahertz (GHz) frequency range. Nucleation of vortices in a superconductor below the first critical field can be assisted by transverse sound in the gigahertz frequency range. Vortices will enter and exist in the superconductor at the frequency of the sound. The threshold parameters of the sound, as computed, will show that this effect is within experimental reach.

Local deformations in continuous elastic theory are described by the displacement vector field say $U(r, t)$, and we want to study the effect of transverse sound waves since such waves will create shear deformations of the crystal lattice.

The frequency of ultrasound achievable in experiment can easily be in the ballpark of $f \sim 10^{10} \text{ s}^{-1}$ [5]. A sound of such frequency and amplitude of a few nanometers can

provide $\omega \sim 10^9 \text{s}^{-1}$ that can generate fictitious magnetic fields above \mathbf{H}_{c1} . For practical purposes, it may be convenient to loosen the restriction on the frequency and amplitude of ultrasound by applying an external magnetic field \mathbf{H} near, but less than \mathbf{H}_{c1} . We shall see that within 1% of \mathbf{H}_{c1} , vortices can be ignited by the ultrasound in the gigahertz frequency range.

1.6 Objectives

- i) To examine the process of vortex entry into and exit from a superconductor and the conditions under which this process occurs.
- ii) To determine the amplitude, velocity and frequency of the ultrasound that can be used to nucleate superconducting vortices.
- iii) To determine the magnetic field \mathbf{B} , generated by the sound at the core of the system.

CHAPTER TWO

LITERATURE REVIEW

2.1 Introduction

Superconductivity is the vanishing of the electrical resistance of a conductor at very low temperatures. It was discovered by Kamerlingh Onnes in 1911 [8] at Leiden, Holland, who found that when the temperature of pure frozen mercury was reduced below 4.2 K, its electrical resistance disappeared resulting in the flow of electrical currents of the order of 10^5 amperes [9]. The phenomenon of superconductivity is manifested in the vanishing of the electrical resistance at a finite temperature called the critical temperature, T_c [2].

Superconductivity is a phenomenon occurring in certain materials, such as mercury, at low temperatures and is characterized by the complete absence of electrical resistance and the damping of the interior magnetic field (Meissner Effect) [7]. Interestingly, adding impurities to mercury did not destroy superconductivity, so that the original reasons for which Kamerlingh – Onnes chose mercury turned out to be unimportant [2]. In 1933, Meissner and Ochsenfeld [7] discovered that a metal cooled in the superconducting state in a moderate magnetic field expels the magnetic field from its interior. This is called the Meissner effect and it shows that such a superconducting material is diamagnetic [2].

For homogenous single crystals of pure metals, the transition width is narrow, about 0.001K, but it gets broadened for polycrystalline or impure materials. The onset is generally taken to be the temperature where the resistance has dropped by 10% when the transition is complete. The resistance becomes indistinguishable from zero [10, 11]. Superconductivity occurs in a wide variety of materials, including simple elements like

tin and aluminum, various metallic alloys, some heavily-doped semiconductors, and certain ceramic compounds containing planes of copper and oxygen atoms. The superconductivity exhibited by metals, alloys and doped semiconductors is nowadays called conventional superconductivity [2, 4, 8, 11]. The latter classes of compounds, known as the Cuprates, are high-temperature superconductors [4].

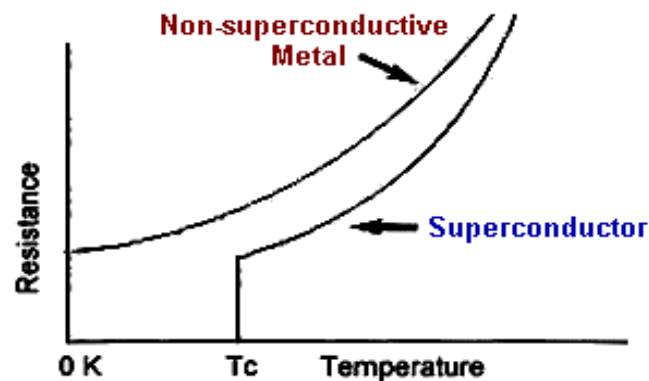


Figure 2.1: Graph of resistance versus temperature for both conductors and superconductors. T_c is the Critical Transition Temperature [9]

Superconductivity does not occur in noble metals like gold and silver. In early developments on the theories of superconductivity, it was thought that ferromagnetism and superconductivity cannot co-exist. However, recently it has been discovered experimentally and theoretically that ferromagnetism and superconductivity can co-exist [12].

In conventional superconductors, superconductivity is caused by a force of attraction between certain conduction electrons arising from the exchange of phonons. This causes the conduction electrons to exhibit a super fluid phase composed of correlated pairs of electrons. There also exists a class of materials, known as unconventional

superconductors, that exhibit superconductivity but whose physical properties contradict the theory of conventional superconductors. In particular, the so-called high-temperature superconductors exhibit superconductivity at temperatures much higher than should be possible according to the conventional theory (though still far below room temperature.) There is currently no complete theory of high-temperature superconductivity [12, 13].

2.2 Microscopic Theory of Superconductivity

Superconductivity has always been a very fascinating but difficult problem for theoretical physicists. It was not until 1957, when an acceptable microscopic theory for superconductivity, based on the concept of pairing of electrons of opposite spins and momenta (time reversed states) near the Fermi surface, was given by Bardeen, Cooper and Schrieffer (BCS) [3].

The mystery of superconductivity was solved and the formulation of the theory brought further progress in the field. The discovery of the isotope effect clearly indicated that, in an explanation of the phenomenon of superconductivity, the interaction between electrons and the crystal lattice must be taken into account. This interaction leads to an attraction between the electrons in a superconductor [9, 14].

The BCS theory explains superconductivity at temperatures close to absolute zero [3, 11]. Cooper realized that atomic lattice vibrations were directly responsible for unifying the entire current. They forced the electrons to pair up into teams that could pass all of the obstacles which caused resistance in the conductor. These teams of electrons are known as **Cooper pairs**. Cooper and his colleagues knew that electrons which normally repel each other must feel an overwhelming attraction in superconductors. The answer to this

problem was found to be in phonons (packets of sound waves present in the lattice as it vibrates) [4, 14].

An electron moving in a metal deforms, or polarizes, the crystal lattice by means of electric forces. The displacement of the ions in the lattice caused in this way affects the state of the other electron, since the latter now finds itself in the field of the polarized lattice with a somewhat altered structure. This results in an effective attraction between the electrons [9, 14].

According to the theory, as one negatively charged electron passes by positively charged ions in the lattice of the superconductor, the lattice distorts. This in turn causes phonons to be emitted which form a trough of positive charges around the electron. Before the electron passes by and before the lattice springs back to its normal position, a second electron is drawn into the trough [9, 13].

It is through this process that two electrons, which should repel one another, link up. The appearance of the attractive force can as well be visualized as follows; As a result of the deformation of the lattice, an electron is surrounded by a 'cloud' of positive charge which is attracted to the electron. The magnitude of this positive charge can exceed the electron charge. Then this electron together with the surrounding 'cloud' represents a positively charged system which will be attracted to another electron [14].

The attractive forces between the electrons due to exchange of phonons can screen the Coulomb repulsion between electrons. The electron pairs are coherent with one another as they pass through the conductor in unison. The electrons are screened by the phonons and are separated by some distance. When one of the electrons that make up a Cooper

pair passes close to an ion in the crystal lattice, the attraction between the negative electron and the positive ion causes a vibration to pass from ion to ion until the other electron of the pair absorbs the vibration. The net effect is that the electron has emitted a phonon and the other electron has absorbed the phonon. It is this exchange that keeps the Cooper pairs together. It is important to understand, however, that the pairs are constantly breaking and reforming [12, 13].

The BCS theory [3] successfully shows that electrons can be attracted to one another through interactions with the crystalline lattice. This occurs despite the fact that electrons have the same charge. When the atoms of the lattice oscillate as positive and negative regions, the electron pair is alternatively pulled together and pushed apart without a collision. The electron pairing is favorable because it has the effect of putting the material into a lower energy state. When electrons are linked together in pairs, they move through the superconductor in an orderly fashion [13].

As long as the superconductor is cooled to very low temperatures, the Cooper pairs stay intact, due to the reduced molecular motion. As the superconductor gains heat energy the vibrations in the lattice become more violent and break the pairs. As they break, superconductivity diminishes. Superconducting metals and alloys have characteristic transition temperatures from normal conductors to superconductors called **Critical Temperature** (T_c). Below the superconducting transition temperature, the resistivity of a material is exactly zero. Superconductors made from different materials have different T_c values [10, 12].

At high temperatures, sufficiently intense thermal motion pushes particles apart from each other and washes away the ion 'coat', which effectively reduces the attractive forces. At low temperatures, however, these forces play a very important role. The crystal lattice is thus the medium which makes the dielectric permittivity in a superconductor negative. The appearance of the additional interelectron attraction can be described in quantum terms as well. This can be visualized as the emission of a phonon by an electron moving through the lattice and the subsequent absorption of the phonon by another electron. This exchange of phonons is what leads to the additional attraction between electrons [12, 14].

At low temperatures, this attraction in a number of materials (superconductors) prevails over the Coulomb electron repulsion. The electron system turns into a bound unit and finite energy must be expended in order to excite it. The energy spectrum of the electron system in this case will not be continuous. The excited state of the electron system is separated from the ground state by an energy interval or energy gap ΔE . A superconductor does have carriers which can carry the superconducting current. However, these carriers are in a bound state, and finite energy must be expended in order to excite this state (for example by means of incident electromagnetic radiation) [12, 14].

Electrical resistance of a metal is due to the interaction of the moving electron system with the vibrations of the crystal lattice or with impurities. However, when there is a gap in the energy spectrum, quantum transitions in the electron fluid will not always be possible. The electron system will not be excited when it is moving slowly. This implies movement without friction, that is, the absence of electrical resistance [11].

At absolute zero, electrons in a metal occupy energy states up to the Fermi level, E_F . The equation $E(\mathbf{p}) = E_F$ defines the so called Fermi surface in \mathbf{p} -space. In the simplest case, when $E = p^2/2m^*$ (m^* is the electron “effective” mass), the Fermi surface is a sphere. The presence of attraction leads to a restructuring of the Fermi surface because of the appearance of the energy gap. Whereas in a normal metal, the electron energy, referred to the Fermi Surface, is equal to $p^2/2m^* - E_F$, and thus can be arbitrarily small, in superconductors it is described by [9];

$$\epsilon = (\xi^2 + \Delta^2)^{1/2} \quad 2.1$$

From this formula (equation 2.1), it's clear that the minimum energy corresponding to $\xi = 0$, is nonvanishing and is equal to Δ . The electrons in a layer of thickness $\Delta(0)$ near the Fermi surface form bound pairs. The magnitude of the energy gap $\Delta(0)$ (considering systems at absolute temperature) depends on the strength of the electron-phonon coupling parameter λ . This dependence has the following peculiar form;

$$\Delta = 2\hbar \Omega_D e^{-1/\lambda} \quad 2.2$$

where Ω_D is the Debye frequency.

The gap thus increases following a curious exponential law. The function $y = e^{-1/\lambda}$ cannot be expanded in a Taylor series for small x and attempts along the perturbation theory also failed. This formula reflects one of the major stumbling blocks on the road to the theory of superconductivity and this was overcome in the BCS theory [3].

Superconductivity arises as a result of interelectron attraction which possesses peculiar features. An electron in a superconductor will be attracted unequally to all other

electrons. It will 'choose' one specific electron which will have opposite momentum and spin and the interaction between this pair will be strongest. The electron system in a superconductor can be described as consisting of bound pairs of such electrons and the excitation of the electron system can be described as a breakup of such a pair. The quantity $2\Delta(0)$, where $\Delta(0)$ is the energy gap defined by equation 2.2, is the pair binding energy. The state of the electrons in a metal is changing constantly and hence the sets of pairs are also changing continuously [11].

Fermi energy E_F is much larger than the phonon energy $\hbar\omega$ and thus two electrons deep down in the Fermi sea are so constrained by the Pauli principle that they cannot take advantage of the attraction. But if these two electrons are on the Fermi surface or very close to the Fermi surface, they form a bound pair by taking advantage of the attraction. In superconductivity, however, we are not concerned with an isolated pair of electrons but we have to deal with many-electron system in which the wave function of all the electrons must allow for this tendency for pair formation [9].

High temperature superconductors have a layered structure. The carrier motion in this case is quasi two-dimensional which is favorable for pairing. It becomes possible even for carriers far from the Fermi level to bind, leading to a large value of the energy gap. In these materials, the ratio $\Delta(0)/E_F$, which indicates the fraction of the electrons that are paired, is much larger than in conventional superconductors [13]. The superconducting state is characterized by the presence of a gap Δ near the Fermi surface. The momentum spread connected with this is determined by the relation $p_F\delta p/m \approx \Delta$, or $\delta p = m\Delta/p_F$. From the uncertainty relation $\delta p\delta r \approx \hbar$, one can estimate the spatial spread as $\delta r \approx \hbar/\delta p \approx$

$\hbar v_F/\Delta$, where v_F is the Fermi velocity. The coherence length (size of the Cooper pair) is described by the expression

$$\xi_0 = \frac{\hbar v_F}{\pi \Delta} \quad 2.3$$

The quantity ξ_0 characterizes the scale of spatial correlation in a superconductor. Substituting typical values of v_F and Δ , we obtain $\xi_0 = 10^{-4}$ cm [9, 12, 13].

The effective interaction between a pair of electrons (Cooper-pair) results from the virtual exchange of a phonon between the two electrons constituting the pair. Such an interaction is called a phonon-electron interaction and it's attractive when the energy difference $\Delta\varepsilon$, between the electronic states involved, is less than the phonon energy $\hbar\omega$. It is found that the critical temperature for transition to the superconducting state depends on the isotopic mass. This pointed to the understanding that the superconducting transition involved some kind of interaction with the crystal lattice [9].

2.3 Characteristics of Superconductivity.

Most of the physical properties of superconductors vary from material to material, such as the heat capacity and the critical temperature at which superconductivity is destroyed. On the other hand, there is a class of properties that are independent of the underlying material. For instance, all superconductors have exactly zero resistivity to low applied currents when there is no magnetic field present. The existence of these “universal” properties implies that superconductivity is a thermodynamic phase and thus possesses certain distinguishing properties which are largely independent of microscopic details [14].

2.3.1 Zero Electrical Resistance

Suppose we were to attempt to measure the electrical resistance of a piece of superconductor. The simplest method is to place the sample in an electrical circuit, in series with a voltage source V (such as a battery) and measure the resulting current. If we carefully account for the resistance, R of the remaining circuit elements (such as the leads connecting the sample to the rest of the circuit, and the source's internal resistance), we would find that the current is simply V/R . Superconductors are also quite willing to maintain a current with no applied voltage whatsoever, a property exploited in the coils of MRI machines, among others [12].

In a normal conductor, an electrical current may be visualized as a fluid of electrons moving across a heavy ionic lattice. The electrons are constantly colliding with the ions in the lattice and during each collision some of the energy carried by the current is absorbed by the lattice and converted into heat (which is essentially the vibrational kinetic energy of the lattice ions). As a result, the energy carried by the current is constantly being dissipated. This is the phenomenon of electrical resistance [2].

The situation is different in a superconductor. In a conventional superconductor, the electronic fluid cannot be resolved into individual electrons due to existence of Cooper pairs. Due to quantum mechanics, the energy spectrum of this Cooper pair fluid possesses an energy gap, meaning there is a minimum amount of energy, ΔE , which must be supplied in order to excite the fluid. Therefore, if ΔE is larger than the thermal energy of the lattice (given by kT , where k is Boltzmann's constant and T is the temperature), the fluid will not be scattered by the lattice. The Cooper pair fluid is thus a super fluid, meaning it can flow without energy dissipation. Experiments have in fact demonstrated

that currents in superconducting rings persist for years without any measurable degradation [2].

2.3.2 Superconducting Phase Transition

In superconducting materials, the characteristics of superconductivity appear when the temperature, T , is lowered below a critical temperature T_c . The value of this critical temperature varies from one material to another [7, 8, 9, 14]. Conventional superconductors usually have critical temperatures ranging from less than 1 K to around 20 K. Solid mercury, for example, has a critical temperature of 4.2 K. As of the year 2001, the highest critical temperature found for a conventional superconductor was 39 K for magnesium diboride (MgB_2), although this material displays enough exotic properties that there is doubt about classifying it as a "conventional" superconductor [12]. Cuprate superconductors can have much higher critical temperatures: $YBa_2Cu_3O_7$, one of the first cuprate superconductors to be discovered, has a critical temperature of 92 K. Mercury-based cuprates have been found with critical temperatures in excess of 130 K. The explanation for these high critical temperatures remains unknown. Electron pairing due to phonon exchanges explains superconductivity in conventional superconductors but does not explain superconductivity in the newer superconductors that have a very high T_c [9, 12, 13].

The onset of superconductivity is accompanied by abrupt changes in various physical properties which is the hallmark of a phase transition. For example, the electronic heat capacity is proportional to the temperature in the normal (non-superconducting) regime. At the superconducting transition, it suffers a discontinuous jump and thereafter ceases to be linear. At low temperatures, it varies instead as $\exp -\alpha/T$ for some constant α . This

exponential behavior is one of the pieces of evidence for the existence of the energy gap [9].

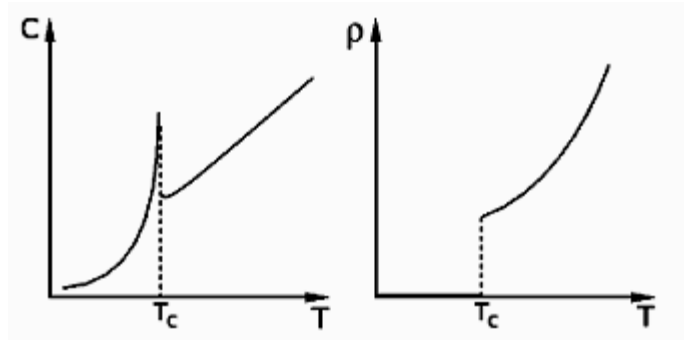


Figure 2.2: Behaviour of heat capacity (C) and resistivity (ρ) at the superconducting phase transition [9].

The order of the superconducting phase transition is still a matter of debate. It had long been thought that the transition is second-order, meaning there is no latent heat. However, recent calculations have suggested that it may actually be weakly first-order due to the effect of long-range fluctuations in the electromagnetic field [9, 14].

2.3.3 Meissner Effect

When a superconductor is placed in a weak external magnetic field \mathbf{B} , the field penetrates for only a short distance λ , called the penetration depth (which is typically of the order 10^{-5} cm), after which it decays rapidly to zero. This is called the Meissner effect and is sometimes thought of as “*perfect diamagnetism*”. For most superconductors, the penetration depth is of the order of a hundred nm [7, 9].

The Meissner effect is sometimes confused with the “perfect diamagnetism” one would expect in a perfect electrical conductor. According to Lenz's law, when a changing

magnetic field is applied to a conductor, it will induce an electrical current in the conductor that creates an opposing magnetic field. In a perfect conductor, an arbitrarily large current can be induced, and the resulting magnetic field exactly cancels the applied field [9].

The Meissner effect is distinct from perfect diamagnetism because a superconductor expels all magnetic fields, not just those that are changing. Suppose we have a material in its normal state, containing a constant internal magnetic field. When the material is cooled below the critical temperature, we would observe the abrupt expulsion of the internal magnetic field, which we would not expect based on Lenz's law. A conductor in a static field, such as the dome of a Van de Graff generator, will have a field within itself, even if there is no net charge in the interior [7].

The magnetic field in a superconductor decays exponentially from whatever value it possesses at the surface. The Meissner effect breaks down when the applied magnetic field is too large i.e. when it goes beyond a critical magnetic field. Superconductors can be divided into two classes (Type I and Type II superconductors) according to how this breakdown occurs. This classification also depends on the transition during the disappearance of electrical resistance. In type I superconductors, the transition is first order (finite latent heat), while in type II superconductors, the transition is second order (no latent heat) with discontinuity in the specific heat [9, 12, 13].

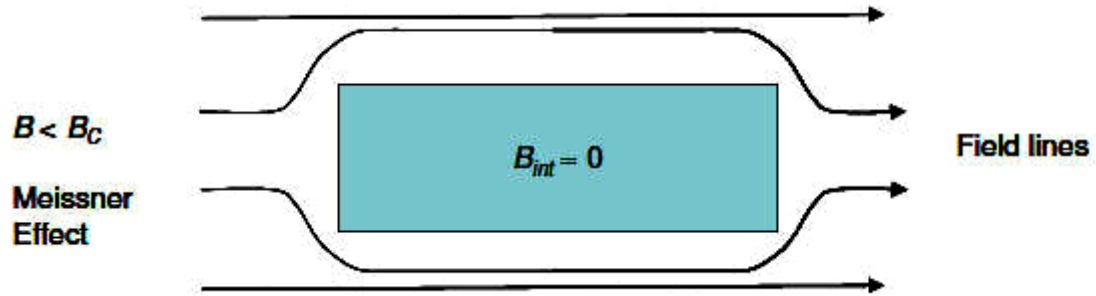


Figure 2.3: The Meissner effect or the expulsion of a magnetic field from a superconductor as it transitions to its superconducting state [12].

The Meissner effect was given a phenomenological explanation by the brothers Fritz and Heinz London [15], who showed that the electromagnetic free energy in a superconductor is minimized provided,

$$\nabla^2 \mathbf{H} = \lambda^{-2} \mathbf{H} \quad 2.4$$

where \mathbf{B} is the magnetic field and λ is the London penetration depth.

This equation 2.4, which is known as the London equation, predicts that the magnetic field in a superconductor decays exponentially from whatever value it possesses at the surface [4, 11, 15].

This critical magnetic field is tabulated for 0 K and decreases from that magnitude with increasing temperature, reaching zero at the critical temperature for superconductivity.

The critical magnetic field at any temperature below the critical temperature is given by the empirical relationship [2].

$$\mathbf{B}_c(T) = \mathbf{B}_c(T = 0) \left[1 - \left(\frac{T}{T_c} \right)^2 \right] \quad 2.5$$

2.4 Types of Superconductors

2.4.1 Type-I Superconductors

In Type I superconductors, superconductivity is abruptly destroyed when the strength of the applied field rises above a critical value H_c . Depending on the geometry of the sample, one may obtain an intermediate state consisting of regions of normal material carrying a magnetic field mixed with regions of superconducting material containing no field. The Type-I category of superconductors is mainly comprised of metals and metalloids that show some conductivity at room temperature [16]. They require incredibly low temperatures to slow down molecular vibrations sufficiently to facilitate unimpeded electron flow in accordance with the BCS theory which suggests that electrons team up in Cooper pairs in order to help each other overcome molecular obstacles, much like race cars on a track drafting each other in order to go faster. Scientists call this process phonon-mediated coupling because of the sound packets generated by the flexing of the crystal lattice. Most pure elemental superconductors (except niobium, Nb) are Type-I Superconductors [4, 9, 12].

2.4.2 Type-II Superconductors.

In Type-II superconductors, raising the applied field past a critical value H_{c1} , leads to a mixed state in which an increasing amount of magnetic flux penetrates the material, but there remains no resistance to the flow of electrical current as long as the current is not too large. At second critical field strength H_{c2} , superconductivity is destroyed. This implies that there is a partial penetration of the magnetic field into the sample when the applied magnetic field H_0 lies between H_{c1} and H_{c2} . The mixed state is actually caused by

vortices in the electronic super fluid, sometimes called fluxons because the flux carried by these vortices is quantized. In superconductivity, a type-II superconductor is characterized by the formation of magnetic vortices in an applied magnetic field and this occurs above H_{c1} . The vortex density increases with increasing field strength. At H_{c2} , superconductivity is completely destroyed. Almost all impure and compound superconductors are Type-II superconductors [16, 17].

The ratio of the London penetration depth, λ to the superconducting coherence length, ξ determines whether a superconductor is type-I or type-II. Type-I superconductors are those with $0 < \lambda/\xi < 1/\sqrt{2}$, and type-II superconductors are those with $\lambda/\xi > 1/\sqrt{2}$ [4].

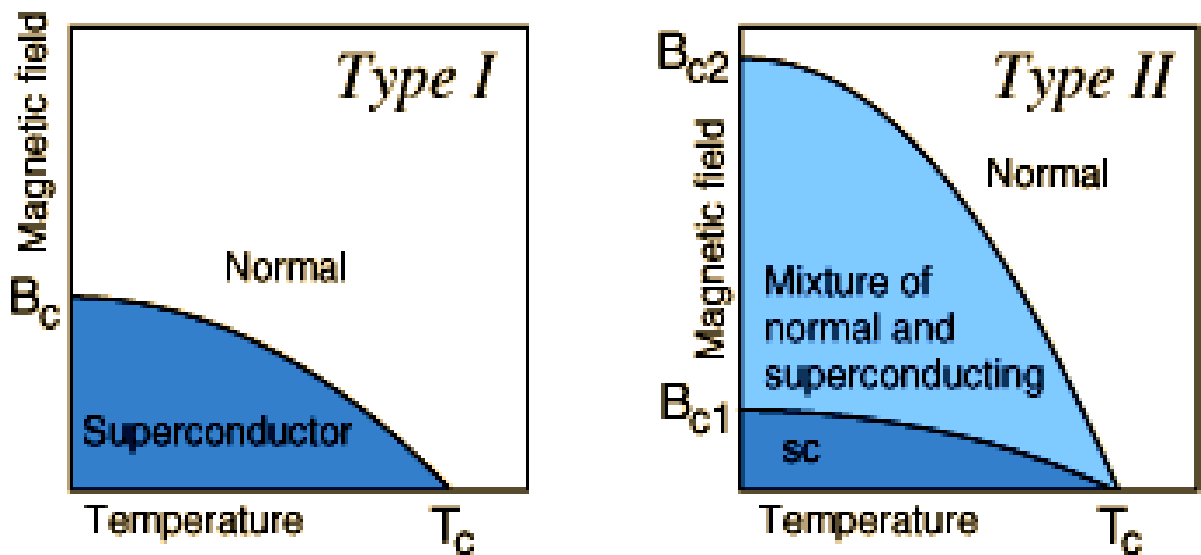


Figure 2.4: Variation of internal magnetic field (B) with temperature (T) for type I and type II superconductors [9].

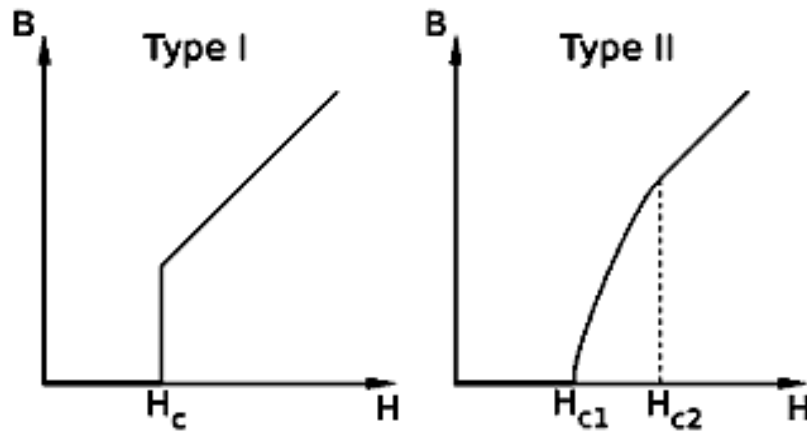


Figure 2.5: Variation of internal magnetic field (B) with applied external magnetic field (H) for type I and type II superconductors [9].

The lower and upper critical fields for the isotropic type-II case are given by [4].

$$H_{c1} = \frac{\Phi_0 \ln K}{4\pi\lambda^2}$$

$$H_{c2} = \frac{\Phi_0}{2\pi\xi^2} \quad 2.6$$

λ is the penetration depth as defined by the London brothers [15].

ξ is the coherence length

$k = \frac{\lambda}{\xi}$ is the Ginzburg – London parameter.

In terms of the thermodynamic critical field,

$$H_c = \frac{\Phi_0}{2\sqrt{2}\pi\lambda\xi}$$

$$H_{c1} = \frac{H_c \ln k}{\sqrt{2\pi}}$$

$$H_{c2} = \sqrt{2k} H_c \quad 2.7$$

The bulk of the material goes normal when the applied magnetic field $H_{app} = H_{c2}$ (superconductivity is completely destroyed) but the superconducting state can persist in a thin surface sheath for H_{app} upto $H_{c3} = 1.7 H_{c2}$ [4].

2.5 Superconducting Vortices

An applied magnetic field H_{app} penetrates a superconductor in the mixed state. Penetration occurs in the form of tubes called vortices that serve to confine a flux. A vortex is a cylinder or tube of magnetic flux containing one quantum of magnetic flux Φ_0 , found in type-II superconductors in the presence of a magnetic field H_{app} . The vortex state is a state where the superconducting and the normal phases coexist. At the center of the vortex, the material is normal and the vortex is circled by a superconducting current carrying a quantized amount of magnetic flux. The motion of vortices generates an electric field, hence energy-dissipation [4].

Type-II superconductors usually exist in a vortex state with normal cores surrounded by superconducting regions. This allows magnetic field penetration. As their critical temperatures are approached, the normal cores are more closely packed and eventually overlap as the superconducting state is lost. The highest field is in the core that has a radius ξ . The core is surrounded by a region of larger radius λ , within which magnetic flux and screening currents flowing around the core are close together. The current

density J_s of these shielding currents decays with distance from the core in an approximately exponential manner [4].

The equation 2.8 provides us with an expression of the magnetic flux passing through a region.

$$\int \mathbf{B} \cdot d\mathbf{S} + \frac{\mu_0}{e^2} \int \frac{\mathbf{J} \cdot d\mathbf{l}}{r^2} = n\Phi_0 \quad 2.8$$

Where n is the number of vortex cores enclosed by the integrals. For an isolated vortex, $n=1$ because it is energetically more favorable for two or more quanta to form separate vortices rather than to exist together in the same vortex [12]. Integration of \mathbf{B} over the cross-sectional area of an isolated vortex from $r = 0$ to $r = \infty$, is numerically equal to the flux quantum Φ_0 and the line integral vanishes because J becomes negligibly small at large distances.

$$\int \mathbf{B} \cdot d\mathbf{A} = \Phi_0, \quad 2.9$$

And it equals the flux quantum $\Phi_0 = 2.00 \times 10^{-7} \text{ G cm}^2$, which is also equivalent to

$$\Phi_0 = \frac{h}{2e} = 2.10 \times 10^{-15} \text{ Tm}^2 \quad 2.10$$

This flux quantum Φ_0 is associated with the Hall effect quantum of resistance R_H

$$R_H = \frac{h}{e^2} = \frac{2\Phi_0}{e} = 25,813 \Omega \quad 2.11$$

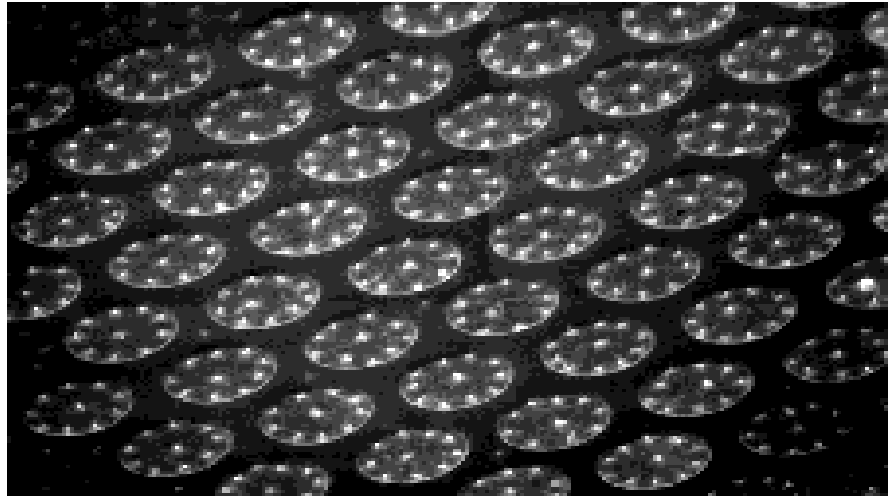


Figure 2.6: Superconducting Vortices (white spots) as imaged by the magnetic decoration technique [14].

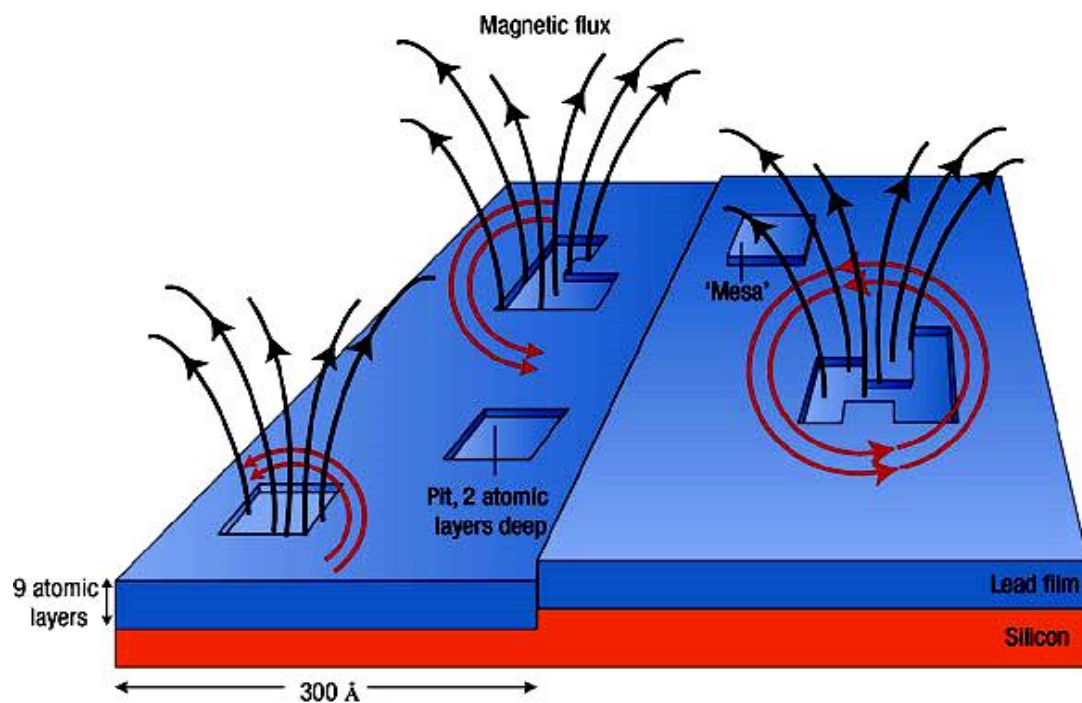


Figure 2.7: Illustrates that magnetic field lines (black) can only penetrate a superconductor through a vortex surrounded by supercurrent flow (red) [14].

Where the London penetration depth λ is larger than the coherence length ξ , there is a possibility of flux penetration inside the sample for magnetic field greater than H_c [10, 11]. Also when the penetration depth is much larger than the coherence length, as is the case with high temperature superconductors, there is considerable overlap of vortices throughout most of the mixed state range, and the magnetic flux is present mainly in the surrounding region, rather than in the actual cores. There is no limit to the length of a vortex. Along the axis, which is also the applied field direction, the magnetic field lines are continuous, thus the flux does not begin and end inside the superconductor, but instead enters and leaves at the superconductor surface, which is also where the vortices begin and end [4, 12].

The magnetic behaviour of a type-II superconductor arises from its vortex structure. Between H_{c1} and H_{c2} , the sample exists in a mixed state (of normal and superconductors) [9]. The field penetration in this mixed state occurs in the triangular lattice of flux vortices. A flux vortex is a normal core of radius ξ (coherence length) and carrying a quantum of magnetic flux Φ_0 , surrounded by vortices of super currents spread over a distance λ [10, 11].

Vortices arrange themselves in a hexadic pattern separated by a distance d , where $\frac{1}{2} \sqrt{3d^2}$ is the area occupied per vortex. Such a structure has been observed on the surface of classical as well as high- T_c superconductors. The magnetic flux of an individual (isolated) vortex is determined by integrating its magnetic field over its area. Near H_{c1} , $d \approx 2\lambda$ and near H_{c2} , $d = 2\xi$ [12]. Near H_{c2} , the vortex cores almost overlap and the flux in each core approaches Φ_0 . Average field inside the superconductor is [4, 12].

$$\mathbf{B}_{\text{in}} = \frac{\Phi_0}{\frac{1}{2}\sqrt{3}d^2} = N_A \Phi_0 \quad 2.12$$

where N_A is the number of vortices per unit area [2].

2.6 Vortices near Lower Critical Field.

When the flux first penetrates the superconductor at $\mathbf{H}_{\text{app}} = \mathbf{H}_{c1}$, the vortices are near the surface and isolated. As the applied field increases, more vortices enter and their mutual repulsion and tendency to diffuse causes them to migrate inwards. Eventually they become sufficiently dense and close enough to experience each other's mutual repulsive forces, so they begin to arrange themselves into a more or less regular hexagonal pattern [12, 13]. For this case we can find the average internal field as

$$\langle \mathbf{H}_{\text{in}} \rangle = \mathbf{H}_{c1} \frac{8\pi \lambda^2}{\sqrt{3} \ln k d^2} \quad 2.13$$

Therefore the separation of vortices when the average internal field equals the lower critical field is given by [4, 13]

$$d = 2 \left(\frac{\pi}{\sqrt{3} \cdot \frac{1}{2} \ln k} \right)^{\frac{1}{2}} \lambda \quad 2.14$$

$$d = \frac{3.81}{\sqrt{\ln k}}, \quad \langle \mathbf{B}_{\text{in}} \rangle = \mathbf{B}_{c1} \quad 2.15$$

Since $\sqrt{\ln 10} = 1.52$ and $\sqrt{\ln 100} = 2.15$, the value of k does not have much effect on the separation of the vortices [4, 13].

2.7 The Mixed State

Between H_{c1} and H_{c2} , a type-II superconductor is in a mixed state, first described by Abrikosov [17] in 1957. The field penetration in the mixed state occurs in the form of a triangular lattice (termed as a flux line lattice, FLL) of flux vortices. At H_{c1} , the first flux vortex is nucleated and with increasing field, their equilibrium (flux vortex of a normal core and vortices of super current) separation is reduced such that at H_{c2} , the normal cores begin to overlap and therefore the bulk of the material turns non- superconducting [2, 10, 11].

2.8 Critical Current in the Mixed State

The most attractive property of a type-II superconductor is its large upper critical field and it is this property which invites its use for making superconducting electromagnets producing lossless high magnetic fields. But, for this application, a superconducting wire must have a large value for H_{c2} , and must also possess the ability to carry a high transport current without resistance in a transverse magnetic field [4, 10, 11].

The resistance-less current in a homogenous type – II superconductor is limited to that value which just produces the field H_{c1} at its surface such that $H_{c1} = \frac{2I_c}{a}$ where ‘a’ is the radius of the wire. Above H_{c1} , the sample contains both the transport current and magnetic vortex lines threading through bulk of the sample [4, 10,11].

Their coexistence results in what [4] is known as the Lorentz driving force F_L given by (equation 1.4)

$$F_L = \frac{1}{c}(\mathbf{B} \times \mathbf{J})$$

This force acts on flux vortices, where \mathbf{J} is the current density and \mathbf{B} is the average magnetic induction [4, 11].

This force F_L is maximum when the transport current is transverse to the magnetic field and it acts on flux vortices, tending them to move. The situation with longitudinal magnetic field is more complicated. Flux vortices take up helical configuration and in doing so reduce F_L such that $F_L \rightarrow 0$ ($\mathbf{B} \times \mathbf{J} = \mathbf{B}J \sin 0$) when \mathbf{B} and \mathbf{J} are in the same direction [10, 11].

This ‘force free’ configuration results in much high \mathbf{J}_c values than in the transverse field case. In a homogenous wire, there is no counteracting force preventing this and an unstable situation results in which the flux vortices are driven into motion. Such a motion is a dissipative process giving rise to resistance and when this occurs, the wire ceases to be of practical interest. Hence, to carry a large current without resistance, the flux vortices must be pinned so that their motion is inhibited. The pinning forces counteract the Lorentz driving force and promote a nonequilibrium vortex distribution. The mixed state can now carry lossless transport current upto a maximum or critical value which corresponds to the driving force being just equal to the pinning force [10, 11].

2.9 Role of Inhomogeneities

For a superconductor to sustain large transport current density in the mixed state, the flux vortices, or more correctly, the flux line lattice (FLL) [4] must be pinned. The pinning can occur through their interaction with various types of microstructural inhomogeneities, such as dislocation networks, different types of inter and intra – grain boundaries, composition fluctuations, precipitates of a second phase e.t.c. They give rise to local

variations in superconducting properties where the flux line energy is locally reduced to get pinned [4, 10, 11].

A flux vortex has basically two components contributing to its line energy: i) the normal core of radius ξ and ii) vortices of circulating super currents spread over a distance. The former leads to the core interaction, while the latter to the magnetic interaction. Generally magnetic pinning is more important in the low-k materials [10, 11]. The interaction between an isolated defect and FLL results in the elementary pinning force F_p which when properly summed up over all the pinning entities per unit volume, taking into account the elastic properties of FLL, gives rise to the volume pinning force $F_p = \frac{-B}{4\pi} \frac{dB}{dx}$.

The critical current density J_c is defined by the force balance equation;

$$F_L = \frac{1}{c} (\mathbf{B} \times \mathbf{J}) = -F_p$$

2.16

However, when the driving force just exceeds the pinning force, the depinning occurs and the current reaches the critical value. Depinning process can also get accelerated by thermal activation [10, 11].

Since most superconducting samples are full of pinning sites (grain boundaries, twin plates, dislocations, impurities, cracks) and since the pinning of vortices is crucial in many applications, this research includes such effects. Various scales of pinning sites can be introduced. One possible scenario is that of many small pinning sites outnumbering the vortices. In this case it is conjectured that a vortex will not move until the current exceeds a certain critical value, the depinning current \mathbf{J}_{pin} , required to break it away from its pinning site. Once moving, the direction of the velocity of the vortex will follow the

Lorentz force as defined in equation 1.4, but the presence of a sea of pinning sites will also slow the vortex to be beneath its ideal speed. Once the depinning current has been exceeded, the velocity may again be linear in the current density or it may be that the curve asymptotes to the ideal curve (as shown in figure 2.8) as the pinning sites have a lesser effect on fast moving vortices [18].

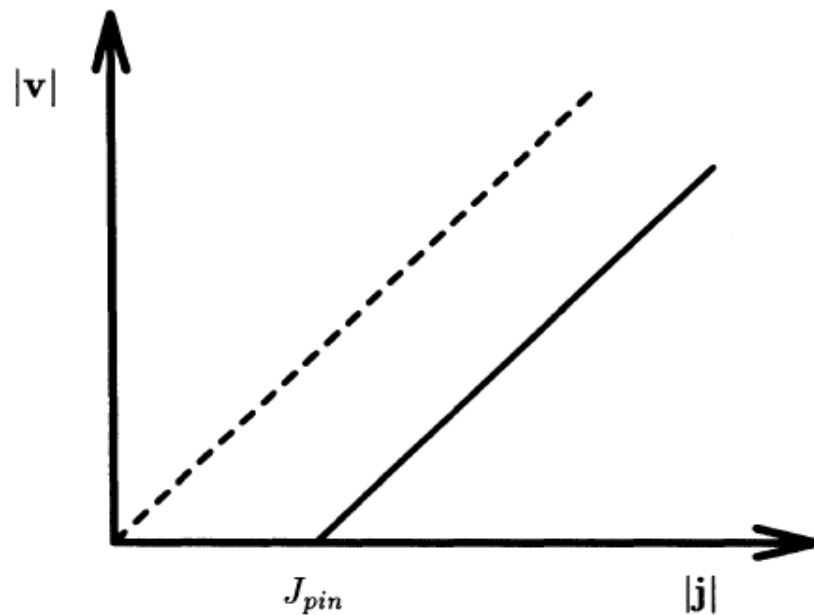


Figure 2.8: The possible form of the velocity of a vortex v as a function of the local current density j . [18]

If the density of the pinning sites is non-uniform throughout the sample, then the depinning current will be a function of position. It will also be a function of temperature [18].

2.10 Nucleation of Superconducting Vortices

When the applied magnetic field is spatially homogeneous and close to H_{c3} , a superconducting layer or sheath nucleates on a portion of the surface at which the applied field is tangential to the surface. Superconductivity nucleation phenomenon for superconductors under applied magnetic fields close to the upper critical field H_{c3} has been studied by many authors. Physicists Saint-James and De Gennes [SdG] were the first to study the surface nucleation phenomenon for a semi-infinite super-conductor occupying the half space and placed in an applied magnetic field which is parallel to the surface of the superconductor [4].

In the case of non-homogeneous applied magnetic fields, interior nucleation may occur first when the applied field is decreased below the upper critical field. More precisely, superconductivity may remain only in the region away from the lateral surface and the order parameter concentrates at the minimum points of the applied magnetic field [9].

For type II superconductors, a third state exists which is known as the mixed state. The mixed state as the name suggests is neither wholly superconducting nor wholly normal but consists of many normal filaments embedded in a superconducting matrix. Each of these filaments carry with it a quantized amount of magnetic flux and is circled by a vortex of superconducting current, thus these filaments are known as vortices. The transition between the normal state and the superconducting state takes place via a bifurcation as the magnetic field is lowered through the second critical value H_{c2} . This bifurcation is subcritical for type-I superconductors and supercritical for type – II

superconductors, hence although the mixed state exists in type-I superconductors, it is unstable and observed only in type-II superconductors [18].

The critical field H_{c1} (the lower critical field) is calculated on the basis of an energy argument; it is the field at which the energy of a wholly superconducting solution becomes equal to the energy of the single vortex solution for an infinite superconductor. There is a barrier to the nucleation of the vortices and that there exists a ‘superheating field’ H_{sh} , such that for fields $H_o < H_{sh}$, vortices will not be generated even though the wholly superconducting solution may not be the minimum energy solution [18].

It has been determined experimentally in [19, 20] and has been examined theoretically in [21] that no vortices will be generated at the boundary until the current density there reaches a critical value \mathbf{J}_{nuc1} , which we call the nucleation current density and which is a material parameter which will depend among other things, surface roughness. When the current density is high enough to generate vortices at the boundary, then the rate of production of vorticity i.e. the flux of the vorticity through the boundary will be proportional to the excess of the current density over the nucleation current density [18].

2.11 Nucleation of Vortices through Mechanical Rotations

Vortices constitute the most relevant topological defects in physics. They consist in a twist of the phase of a wave function around an open line and they are typically associated with a rotation of a fluid, whatever the fluid is made up of (real fluids, optical fluids, and quantum fluids [22]). Vortices are one of the means by which quantum systems acquire angular momentum and react to perturbations of the environment. They have already been predicted, observed and studied in the superfluid phase of helium and are

indeed known to be the key in some important processes in the systems, such as dissipation, moments of inertia and breakdown of super fluidity [23].

In recent experiments performed by Madison and co-workers [24], vortices are created by rotating and elongated trap that is slightly deformed along its transverse dimensions. After this preparation, the trap is switched off and the condensate expands until vortices become directly observable [23].

In these experiments there are several controversial points which are (i) vortices first nucleate at a trap rotation speed or critical frequency larger than that required to stabilize a vortex line in the Thomas-Fermi Theory [25]; (ii) when seen from the top, vortex cores seem partially filled, and (iii) after the nucleation of the first vortex, the angular momentum grows continuously with the rotation speed (not only with discontinuous jumps). In such elongated traps, there exists a mechanism that prevents the nucleation of vortices unless the condensate rotates much faster than the speed required to make one or more vortices energetically stable [23].

Straight vortex lines are locally stable only for very large angular speeds – well beyond the values at which higher vorticities become preferable. It is found that the longitudinal deformation of these topological defects is responsible for an almost continuous growth of the angular momentum with respect to the angular speed. It is difficult to observe the bending of vortex lines in current experimental set ups, since condensates are expanded too much along their transverse dimensions [23]. Before the de-stabilization of the vortexless state, the vortex nucleation process is prevented and the condensate may only

adapt to the rotation speed by means of transverse deformations that are described in [26].

In recent numerical work, Butts and Rokhsar [27] observed that with increasing angular frequency of the external rotation, a sequence of phase transitions occurs between configurations with different vortex structures. Stable configurations correspond to vortex distributions with some particular symmetry and survive within specific intervals of rotational frequency and between ‘magic’ values of the angular momentum, which is not quantized. After the first vortex penetrates the trap in a second-order phase transition, the trap center becomes a crystallization center of vertical Wigner molecules [28] of increased complexity. As the rotational speed increases, the growing aggregates acquire new elements, making them more and more similar to the infinite lattice. Such elements penetrate the trap via phase transitions which are most likely of the first order if symmetry is changed. The symmetry index of the vertical molecules remains a kind of ‘motion integral’ [29]. It replaces the angular momentum which is not conserved [27].

The use of acousto-optic deflection to generate smooth rotation of an optical lattice at a well defined frequency has allowed the exploration of a new method of vortex nucleation. For deeper lattices in which the system is split into well localized condensates, a linear dependence of vortex number on optical lattice has been observed for rotational frequencies below the thermodynamic critical frequency for vortex nucleation which implies that vortices are created locally at a lattice plaquette [30].

CHAPTER THREE

METHODOLOGY

3.1 Introduction

A superconducting cylinder rotated at an angular velocity of 10^9s^{-1} will have superconducting vortices enter the bulk of the cylinder [5]. However, as discussed in chapter two of this thesis, it is not experimentally possible to attain such a high value for a mechanical rotation. The alternative method could be to generate local rotations in a superconductor by high frequency ultrasound resulting into the possibility of the nucleation of a vortex by sound.

This chapter examines the process of vortex entry into and exit from a superconductor and the conditions under which this process occurs. Calculations will also be done to show how sound enters the problem. Finally, an equation for the angular velocity, Ω of a rotating superconducting slab of thickness d , will be derived.

3.2 Nucleation of Superconducting Vortices

The process of vortex entry into and exit from a superconductor can occur in a surface sheath similar to the one that remains superconducting for applied fields in the range $\mathbf{B}_{c2} < \mathbf{B}_{app} < \mathbf{B}_{c3}$ [4].

For a vortex to enter a superconductor, the Gibb's free energy ($G = H - TS$) of the system must be lowered. The extra free energy due to the vortex has to be calculated and the condition at which it becomes negative has to be determined. It should be understood that the system under consideration is dynamical and thus not thermodynamically in equilibrium. However, we are interested in the free energy of Cooper pairs which can

adjust to the changes of state in a time scale orders of magnitude shorter than the period of sound. This time scale is proportional to the relaxation time $\tau = 10^{-12}$ s of the Cooper pairs [9].

The period of the sound $T = 1/f$ will always be greater than 10^{-10} s. Under these conditions, the system will be adiabatic and the thermodynamic equilibrium can be easily established. We now have to do calculations that will show how the sound enters the problem [5].

It is convenient to calculate the extra free energy in terms of the magnetic field and its spacial derivatives. The electric field produced by the time derivatives will be neglected.

Kinetic energy of the superfluid is $\frac{1}{2} n_s m v^2$, where n_s is the number density of the superconducting electrons and \mathbf{v} is the velocity of the Cooper pairs which is given by [4, 5]:

$$\mathbf{V} = \frac{e^*}{m^*} \left(\frac{\hbar c}{e^*} \nabla \phi - \mathbf{A} \right) = \frac{\hbar}{m^*} \nabla \phi - \frac{e^*}{m^*} \mathbf{A} \quad 3.1$$

Where ϕ and \mathbf{A} are the phase of the superfluid and the magnetic vector potential respectively,

$m^* = 2m$ = effective mass of the Cooper pairs.

$e^* = 2e$ = effective charge of the Cooper pairs.

It is important to note that superfluids such as helium are able to flow below lambda point (2.17 K) without viscous drag and without heat dissipation [12]. Normal electrons experience viscous forces as they move relative to the nuclei contributing zero average

normal current. The ionic charge per unit volume consisting of all the nuclei and the normal electrons is therefore exactly opposite to that of the Cooper pairs. Total current is then;

$$\mathbf{J} = en_s(\mathbf{v} - \dot{\mathbf{u}}) \quad 3.2$$

Equation 3.2 reflects the fact that the electric current corresponds to the motion of electrons relative to ions. This is invariant with respect to the motion of the reference frame. With equation 3.1, we can express the gauge invariant current in terms of ϕ and $\dot{\mathbf{u}}$ as;

$$\mathbf{J} = \frac{n_s e \hbar}{2m} \left(\nabla \phi - \frac{2e}{\hbar c} \mathbf{A}_{\text{eff}} \right) \quad 3.3$$

Where \mathbf{A}_{eff} is the effective vector potential felt by the electrons in the rotating frame of the ions [30] and is given by,

$$\mathbf{A}_{\text{eff}} = \mathbf{A} + \frac{mc}{e} \dot{\mathbf{u}} \quad 3.4$$

Using equation 3.3, the total kinetic energy of the superconducting electrons may be expressed in terms of the total current \mathbf{j} and derived as follows;

$$\mathbf{j} = en_s(\mathbf{v} - \dot{\mathbf{u}}) = en_s \mathbf{v} - en_s \dot{\mathbf{u}} \quad \text{or } en_s \dot{\mathbf{u}} + \mathbf{j} = en_s \mathbf{v} \text{ or } \mathbf{v} = \left(\dot{\mathbf{u}} + \frac{1}{en_s} \mathbf{j} \right)$$

Kinetic energy of one electron is $\frac{1}{2} m \mathbf{v}^2 = \frac{1}{2} m \left(\dot{\mathbf{u}} + \frac{1}{en_s} \mathbf{j} \right)^2$. Thus the kinetic energy of all the superconducting electrons, n_s (where n_s is the number density) in an element of volume d^3r is,

$$\frac{1}{2} m n_s \left(\dot{\mathbf{u}} + \frac{1}{e n_s} \mathbf{j} \right)^2 d^3 r$$

Thus the kinetic energy of the superconducting electrons in a given volume will be

$$KE_e = \int \frac{1}{2} m n_s \left(\frac{1}{e n_s} \mathbf{j} + \dot{\mathbf{u}} \right)^2 d^3 r \quad 3.5$$

The energy E_s of the sound is given by [3];

$$E_s = \int \frac{1}{2} (\rho_0 \dot{\mathbf{u}}^2 - \lambda_{iklm} u_{ik} u_{lm}) d^3 r \quad 3.6$$

where ρ_0 is the combined mass density of ions and normal electrons, λ_{iklm} is the tensor of elastic coefficients and $u_{ik} = \frac{1}{2} (\partial_i u_k + \partial_k u_i)$ is the strain tensor. Using the Maxwell's equation $\nabla \times \mathbf{B} = \frac{4\pi}{c} \mathbf{j}$ and combining equations 3.5 and 3.6, the expression for the total

Gibb's free energy yields;

$$G = \mathcal{F}_0 + \frac{1}{8\pi} \int \left[\mathbf{B}^2 + \frac{\lambda^2}{f(r)} (\nabla \times \mathbf{B})^2 \right] d^3 r + \frac{1}{4\pi} \int \frac{mc}{e} \dot{\mathbf{u}} \cdot (\nabla \times \mathbf{B}) d^3 r - \frac{1}{4\pi} \int \mathbf{H} \cdot \mathbf{B} d^3 r + \int \frac{1}{2} [\rho \dot{\mathbf{u}}^2 - \lambda_{iklm} u_{ik} u_{lm}] d^3 r \quad 3.7$$

In equation 3.7, \mathcal{F}_0 is the free energy in the absence of currents, fields and sound and λ is London penetration depth given by;

$$\lambda = \sqrt{\left(\frac{mc^2}{4\pi n_s e^2} \right)} \quad 3.8$$

$$f(r) = (|\psi|/|\psi_\infty|)^2 \quad 3.9$$

Where ψ is the complex order parameter and $|\psi_\infty|$ is the order parameter in the absence of gradients and fields and is given by;

$$|\psi_\infty| = \sqrt{(n_s/2)} \quad 3.10$$

The total mass density of the superconductor (mass density of ions, normal electrons and superconducting electrons) is given by the equation 3.11.

$$\rho = \rho_0 + n_s m \quad 3.11$$

The fourth term in equation 3.7 represents the interaction of the external magnetic field \mathbf{H} with the magnetization \mathbf{B} (due to the superconducting currents). It is this term that is responsible for the nucleation of vortices in the absence of sound when $\mathbf{H} \geq \mathbf{H}_{c1}$ [5].

Before we can calculate the free energy given by equation 3.7, we have to first work out the value of the magnetic field. This is done by replacing the current \mathbf{j} in the Maxwell's equation $\nabla \times \mathbf{B} = \frac{4\pi}{c} \mathbf{j}$ by using equation 3.3 and defining the gauge invariant vector potential \mathbf{Q} as

$$\mathbf{Q} = \mathbf{A} - \left(\frac{\hbar c}{2e}\right) \nabla \phi \quad 3.12$$

We then obtain the following equation

$$\lambda^2 \nabla \times (\nabla \times \mathbf{Q}) + f(r) \mathbf{Q} = - \frac{mc}{e} f(r) \dot{\mathbf{u}} \quad 3.13$$

Which is equivalent to;

$$\frac{mc^2}{4\pi n_s e^2} \nabla \times (\nabla \times \mathbf{Q}) + f(r) \mathbf{Q} = - \frac{mc}{e} f(r) \dot{\mathbf{u}} \quad 3.14$$

and

$$(\nabla \times \mathbf{B}) = \frac{2\pi}{cm} n_s e \hbar \nabla \phi - \frac{4\pi e^2 n_s}{mc^2} \mathbf{A} - \frac{4\pi n_s e}{c} \dot{\mathbf{u}} \quad 3.15$$

Equation 3.15 can be rearranged to give equation 3.16 below.

$$-\frac{4\pi n_s e}{c} \dot{\mathbf{u}} = (\nabla \times \mathbf{B}) - \frac{2\pi}{cm} n_s e \hbar \nabla \phi + \frac{4\pi e^2 n_s}{mc^2} \mathbf{A} \quad 3.16$$

Multiplying equation 3.16 by $\frac{mc^2}{e^2}$, yields

$$-\frac{4\pi n_s mc}{e} \dot{\mathbf{u}} = \frac{mc^2}{e^2} (\nabla \times \mathbf{B}) - \frac{2\pi}{e} n_s c \hbar \nabla \phi + 4\pi n_s \mathbf{A} \quad 3.17$$

This then simplifies to:

$$\frac{c^2 m}{2\pi e^2} (\nabla \times \mathbf{B}) - \frac{2n_s c \hbar}{2e} \nabla \phi + 2n_s \mathbf{A} = -\frac{2n_s mc}{e} \dot{\mathbf{u}} \quad 3.18$$

For $\nabla \phi = 0$ ($\mathbf{Q} = \mathbf{A}$), equation 3.13 becomes equivalent to London's equation with a source. When a vortex enters a superconductor, the phase must be quantized according to the condition $\oint \nabla \phi \cdot d\mathbf{l} = 2\pi$. For certainty, we consider a transverse standing sound wave having one node at the centre of a superconducting slab of thickness d large compared to the coherence length ξ . The external field is applied parallel to the slab. In this case $\lambda_s = 2d$. If the field is close to \mathbf{H}_{c1} , a vortex will periodically enter and exit the slab.

For Meissner effect $\mathbf{B} = 0$ and $\nabla \phi = 0$, equation 3.18 reduces to;

$$2n_s \mathbf{A} = -\frac{2n_s mc}{e} \dot{\mathbf{u}} \quad 3.19$$

$$\text{Or } \mathbf{A} = -\frac{2mc}{e} \dot{\mathbf{u}} \quad 3.20$$

Equation 3.20 reflects the condition for the Gibb's free energy to become negative such that the vortices can enter the bulk of the superconductor.

If $A_s(\mathbf{r})$ represents the vector potential for the sound, then the corresponding magnetic field \mathbf{B}_s due to the sound is given by [5];

$$\mathbf{B}_s = \nabla \times \mathbf{A}_s(\mathbf{r}) = -\frac{2mc}{e}(\nabla \times \dot{\mathbf{u}}) = -\frac{2mc}{e}(2\Omega) = -\frac{4mc}{e}\Omega \quad 3.21$$

(v) Velocity (linear) of rotation at the surface of the cylinder is related to the angular velocity, Ω , of the cylinder via $V = \Omega r = \dot{u}$. The wave vector k is given by

$$= \frac{\omega}{v} = \frac{2\pi}{\lambda_s} = \frac{\pi}{d} \quad 3.22$$

Where λ_s is the wavelength of sound ($\lambda_s = 2d$)

Angular momentum $L = \mathbf{r} \times \mathbf{p}$ (momentum) = $\mathbf{u} \times \mathbf{p}$; $k = \frac{p}{\hbar}$; $L = \mathbf{u} \times \mathbf{k}\hbar = \hbar \mathbf{u} \times \mathbf{k}$

$$\Omega = \frac{1}{2}\nabla \times \dot{\mathbf{u}} = \frac{1}{2}\nabla \times (U_o \sin kx)\omega \cos(\omega t)\mathbf{e}_y \quad [3]$$

$$= \frac{1}{2}U_o(U_o \sin kx)\omega \cos(\omega t)\nabla \times \mathbf{e}_y = \frac{\omega}{2}U_o(\sin kx)\cos(\omega t).\mathbf{e}_y$$

$$= \frac{1}{2}\omega u_o k = \frac{\pi U_o}{2d}\omega \quad 3.23$$

Assuming different values for λ_s , we can get different values for d (thickness of the superconducting slab). For different values of U_o , ω and d , equation 3.23 will give different values for Ω . These values of Ω can be used in equation 3.21 to get various values for \mathbf{B}_s the required magnetic field H_{c1} for nucleation of vortices.

CHAPTER FOUR

RESULTS AND DISCUSSION

4.1 Introduction

This chapter involves calculations that will determine the relationship between the ultrasound amplitude U_o , ultrasound angular velocity ω , rotating slab thickness d , ultrasound wavelength λ_s , ultrasound velocity v_s and frequency f_s . The angular velocity, Ω of rotation of a superconducting cylinder will be calculated for different values of slab thickness, d and angular velocity ω . Equation 3.21 will be used to calculate the generated magnetic fields \mathbf{B}_s for different ω , Ω and d .

4.2 Ultrasound amplitude U_o and rotating slab thickness, d .

Table 4.1 shows the values of ultrasound amplitude U_o , velocity ω and the rotating slab thickness d for assumed values of ultrasound wavelength λ_s . The following equations have been used to calculate the slab thickness and ultrasound amplitude.

$$\text{Rotating slab thickness, } d = \frac{\lambda_s}{2}, \quad 4.1$$

From the wave equation $v = \lambda f$,

$$f = \frac{v_s}{\lambda_s} \quad 4.2$$

Where $V_s = 3.3 \times 10^3 \text{ ms}^{-1}$, the speed of ultrasound in the superconducting cylinder.

U_o , the amplitude of the ultrasound, can be calculated using the equation below.

$$U_o = \frac{\epsilon}{4} \left(\frac{d}{\pi \lambda} \right)^4 \frac{\hbar k^2}{mv} \quad 4.3$$

$$\epsilon = 1 - \frac{H}{H_{c1}}, \quad \epsilon \text{ is the electron energy of the superconductor.} \quad 4.4$$

With H within 1% of H_{c1} and k , the wave number, is taken as 2

Table 4.1: Calculated values of ultrasound frequency f_s , thickness d of the rotating superconducting slab and ultrasound amplitude, U_0 using assumed values of ultrasound wavelength, λ_s .

λ_s (m) $\times 10^{-6}$	f_s (Hz) $\times 10^9$	d (m) $\times 10^{-6}$	U_0 (m) $\times 10^{-9}$
0.50	6.60	0.25	0.23
0.80	4.13	0.40	0.23
1.00	3.30	0.50	0.23
1.20	2.75	0.60	0.23
1.50	2.20	0.75	0.23
1.80	1.83	0.90	0.23
2.00	1.65	1.00	0.23
2.50	1.32	1.25	0.23
3.00	1.10	1.50	0.23
3.50	0.94	1.75	0.23

Table 4.1 shows that for different values of the ultrasound wavelength λ_s and thickness, d of the rotating slab, the ultrasound amplitude U_o , as calculated, will always be a constant.

The ultrasound velocity is taken as $V_s = 3.30 \times 10^3$ m/s.

A graph of rotating slab thickness, d against the ultrasound wavelength, λ is plotted to show the relationship between these parameters.

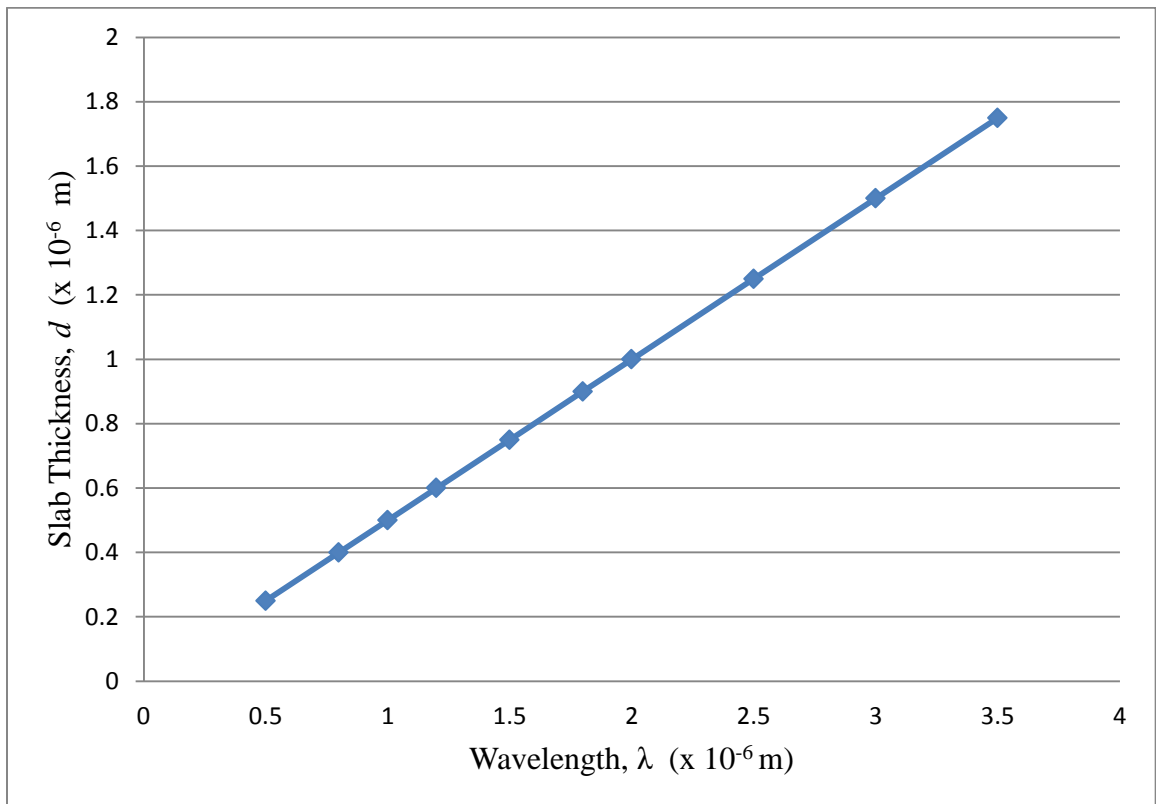


Figure 4.1: The linear relationship between the thicknesses d , of a rotating slab and the wavelength λ , of the ultrasound with constant amplitude of 0.23 nm.

The graph in figure 4.1 indicates a direct linear relationship between the rotating slab thickness and the ultrasound wavelength. In this case, the ultrasound amplitude is held constant at 0.23nm. The gradient of 0.5 of this line indicates that the wavelength of the

ultrasound doubles for every unit increment in the thickness of the rotating slab. The equation of the graph is:

$$\text{Slab thickness, } d = 0.5 \lambda \quad 4.5$$

From equation 4.2 and subsequent calculations in table 4.1, the research has been able to determine ultrasound angular velocities, ω_s , of the order 10^9 s^{-1} . These are values of high frequency ultrasound hence the possibility of nucleation of a vortex by sound.

The research was able to obtain ultrasound frequencies in the range $0.94 \times 10^9 \text{ s}^{-1}$ to $6.60 \times 10^9 \text{ s}^{-1}$ (gigahertz frequency range) and wavelengths in the range $0.5 - 3.5 \mu\text{m}$ as reflected in table 4.1. These parameters of the ultrasound, as computed, show that this effect of nucleation of vortices in a superconductor below the first critical field, H_{c1} , is within experimental reach.

4.3 Rotational angular velocity, Ω of the superconducting cylinder

Using the formula $\Omega = \frac{\pi}{2} \frac{U_0}{d} \omega$ from equation 3.23, we then determine the angular velocity with which a superconducting cylinder is rotated about its symmetry axis.

Table 4.2: Calculated values of angular velocity Ω of a rotating superconducting slab of different values of thickness, d and ultrasound angular velocity, ω_s (as calculated from table 4.1) for constant ultrasound amplitude, $U_o = 0.23\text{nm}$.

d (m) $\times 10^{-6}$	ω_s (Hz) $\times 10^9$	Ω (s^{-1}) $\times 10^6$
0.25	6.60	9.54
0.40	4.13	3.73
0.50	3.30	2.38
0.60	2.75	1.66
0.75	2.20	1.06
0.90	1.83	0.73
1.00	1.65	0.60
1.25	1.32	0.38
1.50	1.10	0.26
1.75	0.94	0.19

From the calculations whose results are shown in table 4.2 , it's evident that as the rotating slab thickness, d , is increased, the angular velocity, Ω of the rotating slab decreases with a decreasing ultrasound angular velocity, ω_s . The ultrasound amplitude U_o is held constant at 0.23 nm.

A graph of rotational angular velocity, ω and superconductor slab thickness is then plotted to further show the relationship.

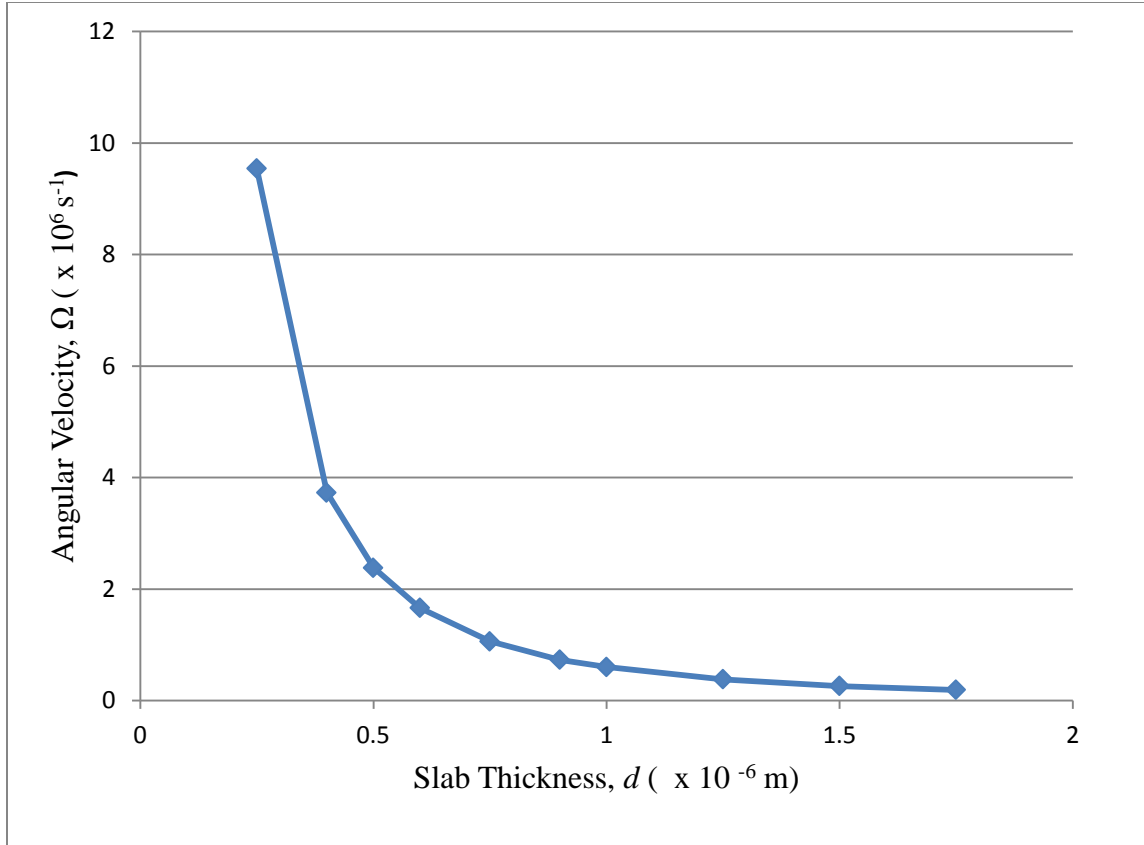


Figure 4.2: Relationship between the angular velocity Ω and the thickness d of a rotating slab of a superconducting cylinder. The ultrasound amplitude is constant, $U_o = 2.3 \times 10^{-10}$ m.

Figure 4.2 shows that the angular velocity, Ω of the rotating superconducting cylinder, will be smaller as its thickness d , increases. This occurs for decreasing values in the ultrasound angular velocity ω_s . The curve is exponential in nature and above a certain value of slab thickness i.e. $1.75 \times 10 \mu\text{m}$, the angular velocity of rotation of the slab is not affected much by increasing its thickness.

4.4 Relationship between angular velocities of the rotating superconducting cylinder and ultrasound.

Table 4.3: Calculated values of angular velocity Ω of a rotating superconducting slab of thickness $d = 0.25 \times 10^{-6}$ m with ultrasound of amplitude, $U_0 = 0.23 \times 10^{-9}$ m and varying angular frequency, ω_s .

ω_s (Hz) $\times 10^9$	Ω (s^{-1}) $\times 10^6$
6.60	9.54
4.13	5.97
3.30	4.77
2.75	3.97
2.20	3.18
1.83	2.64
1.65	2.38
1.32	1.91
1.10	1.59
0.94	1.36

Table 4.3 shows a clearly defined trend of decreasing rotational angular velocity Ω for a slab whose thickness d , is constant at $0.25\mu\text{m}$ and with an ultrasound whose angular velocity ω_s , is also decreasing.

A graph of rotational angular velocity, Ω of the superconducting cylinder is plotted against the ultrasound angular velocity, ω .

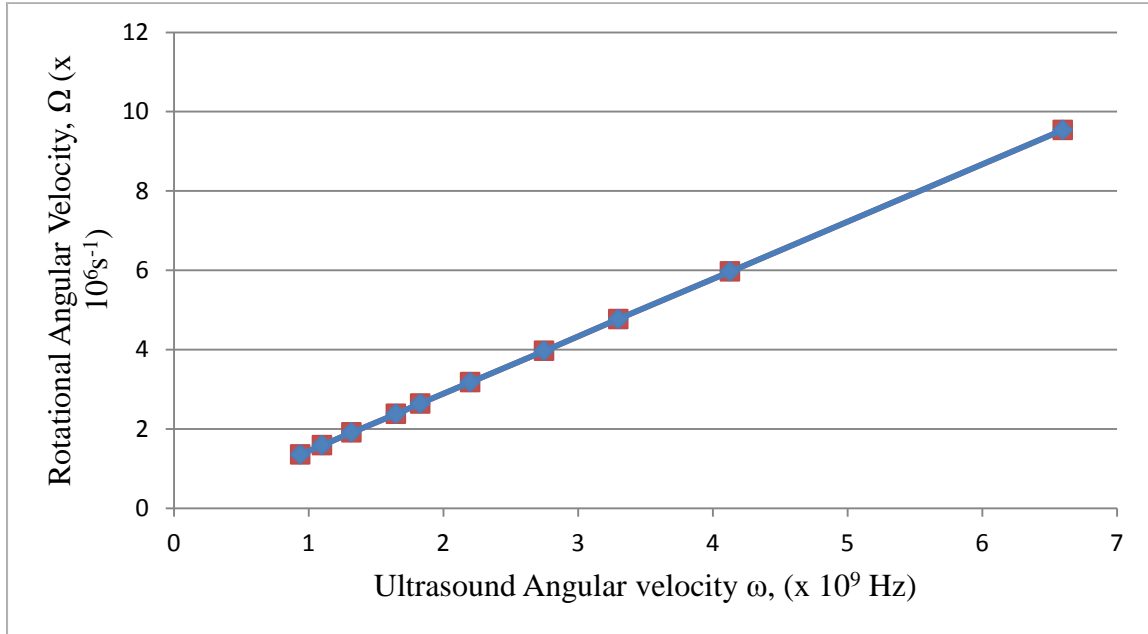


Figure 4.3: Relationship between the rotational angular velocity, Ω of the superconducting slab and the ultrasound angular velocity, ω . The slab thickness, $d = 0.25\mu\text{m}$ and ultrasound amplitude, $U_0 = 0.23 \times 10^{-9}$ m.

The following equation connects the rotational angular velocity, Ω of the superconducting slab and the ultrasound angular velocity, ω for constant ultrasound amplitude U_0 and varying slab thickness, d .

When $U_0 = 0.23$ nm and $d = 0.25 \mu\text{m}$

$$\Omega = 1.445 \times 10^{-3} \omega$$

4.6

Table 4.4: Calculated values of angular velocity Ω of a rotating superconducting slab of thickness $d = 0.75 \times 10^{-6}$ m with ultrasound of amplitude, $U_o = 0.23 \times 10^{-9}$ m and varying angular velocities, ω_s .

ω_s (Hz) $\times 10^9$	Ω (s^{-1}) $\times 10^6$
6.60	3.18
4.13	1.99
3.30	1.59
2.75	1.32
2.20	1.06
1.83	0.88
1.65	0.79
1.32	0.64
1.10	0.53
0.94	0.45

Table 4.4 shows a clearly defined trend of decreasing rotational angular velocity Ω for a slab whose thickness d , is constant at $0.75\mu\text{m}$ and with an ultrasound whose angular velocity ω_s , is also decreasing. However, when compared to table 4.3, it shows that for the same values of ultrasound amplitude U_o and angular velocity ω_s , the rotational angular velocities of the slab are much lower when the slab thickness is increased from $0.25 \mu\text{m}$ to $0.75 \mu\text{m}$. This further confirms results obtained in table 4.2 and figure 4.2.

A graph of rotational angular velocity, Ω of the superconducting cylinder is plotted against the ultrasound angular velocity, ω .

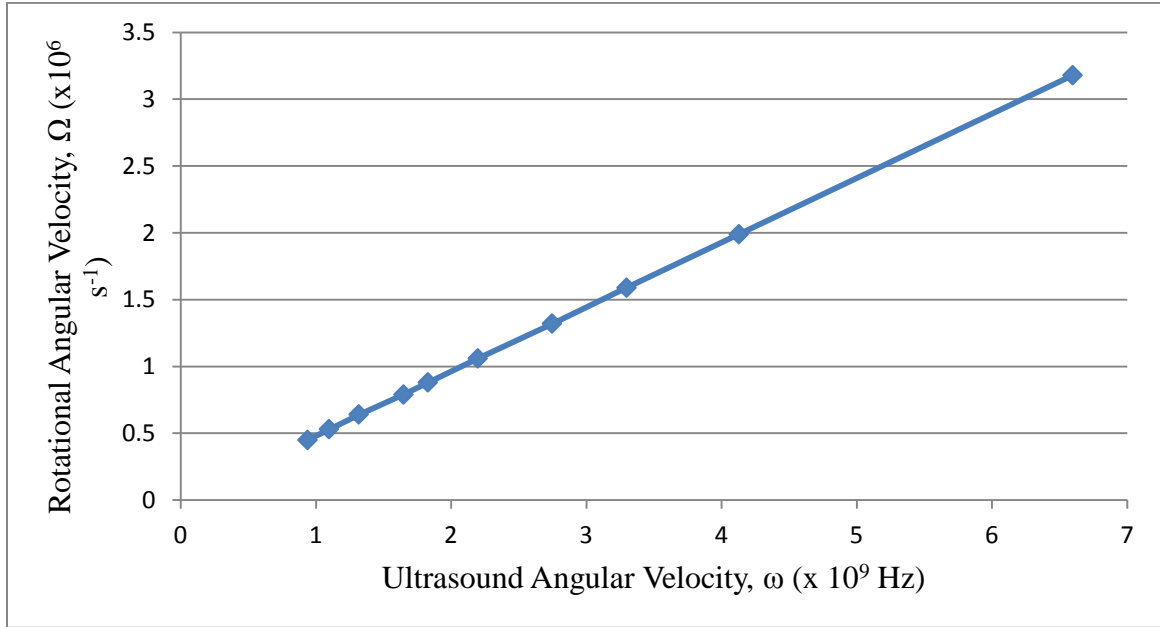


Figure 4.4: Relationship between the rotational angular velocity, Ω of the superconducting slab and the ultrasound angular velocity, ω . The slab thickness, $d = 0.75\mu\text{m}$ and ultrasound amplitude, $U_o = 0.23 \times 10^{-9}$ m.

The following equation connects the rotational angular velocity, Ω of the superconducting slab and the ultrasound angular velocity, ω for constant ultrasound amplitude U_o and varying slab thickness, d .

When $U_o = 0.23$ nm and $d = 0.75 \mu\text{m}$

$$\Omega = 0.482 \times 10^{-3} \omega$$

4.7

Table 4.5: Calculated values of angular velocity Ω of a rotating superconducting slab of thickness $d = 1.75 \times 10^{-6}$ m with ultrasound of amplitude, $U_0 = 0.23 \times 10^{-9}$ m and varying angular velocities, ω_s .

ω_s (Hz) $\times 10^9$	Ω (s^{-1}) $\times 10^6$
6.60	1.36
4.13	0.85
3.30	0.68
2.75	0.57
2.20	0.45
1.83	0.38
1.65	0.34
1.32	0.27
1.10	0.23
0.94	0.19

A graph of rotational angular velocity, Ω of the superconducting cylinder is plotted against the ultrasound angular velocity, ω .

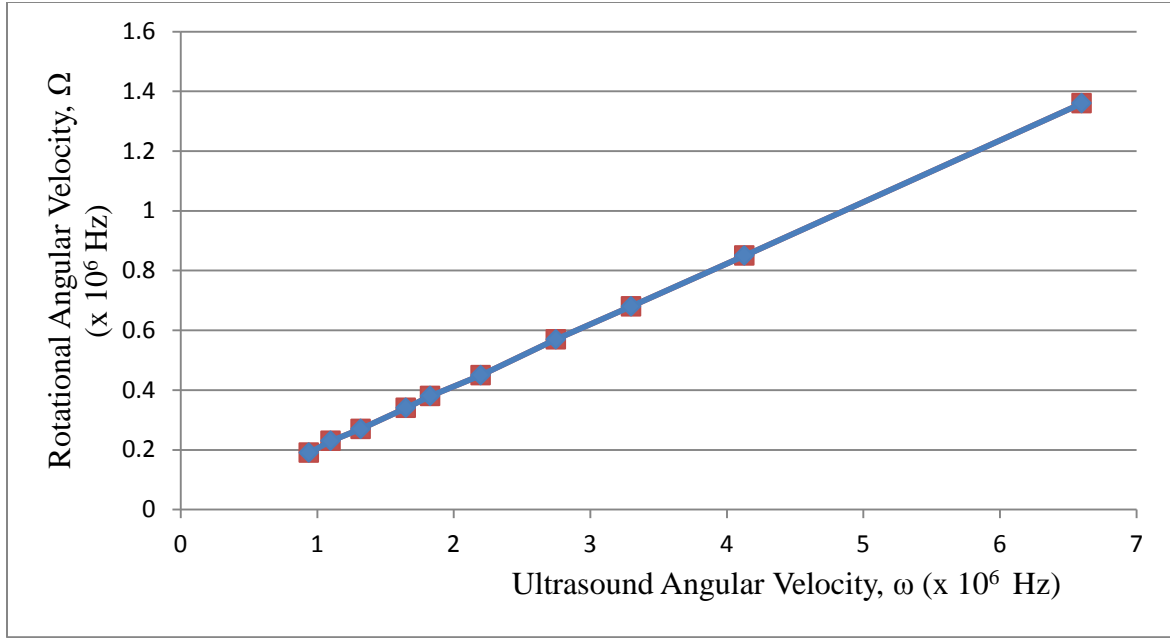


Figure 4.5: Relationship between the rotational angular velocity, Ω of the superconducting slab and the ultrasound angular velocity, ω . The slab thickness, $d = 1.75\mu\text{m}$ and ultrasound amplitude, $U_o = 0.23 \times 10^{-9}$ m.

The following equation connects the rotational angular velocity, Ω of the superconducting slab and the ultrasound angular velocity, ω for constant ultrasound amplitude U_o and varying slab thickness, d .

When $U_o = 0.23$ nm and $d = 1.75 \mu\text{m}$

$$\Omega = 0.23 \times 10^{-3} \omega \quad 4.8$$

Equations 4.6, 4.7 and 4.8 give very important linear relationship between the rotational angular velocity Ω of the superconducting slab and the applied ultrasound angular velocity ω . Equation 3.23 was applied in calculating the values of Ω as shown in tables 4.3, 4.4 and 4.5. The research also notes that the rotating slab thickness, d has an effect on its rotational angular velocity, Ω in which an increase in d results to a decrease in Ω .

Therefore to achieve the high rotational angular velocities desired for the superconducting cylinder, its thickness must be kept very small.

A summary graph of rotational angular velocity, Ω of the superconductor and the ultrasound angular velocity, ω is then plotted for different values of slab thickness, d .

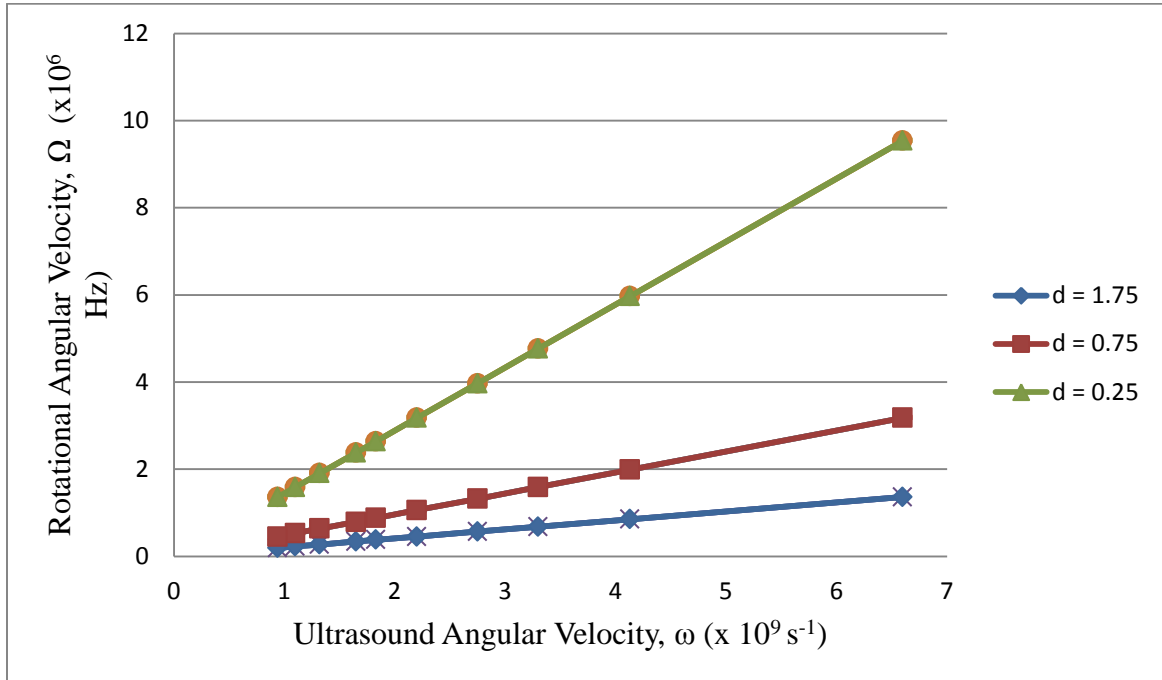


Figure 4.6: Relationship between the rotating superconducting slab thickness d , the angular velocity ω , of the ultrasound (of constant ultrasound amplitude of $U_o = 0.23$ nm.) and the angular velocity, Ω of rotation of the superconducting cylinder.

Figure 4.6 summarises the rotational angular velocities, Ω of the superconducting slab when its thickness is varied from 0.25 to 1.75 μm . A general trend is seen for the same values of ultrasound amplitude U_o and angular velocity ω_s . The rotational angular velocities, Ω of the slab are much higher when the slab thickness is 0.25 μm . Increasing

the slab thickness to 1.75 significantly reduces the rotational angular velocities, Ω obtained. This further confirms results obtained in table 4.2 and figure 4.2.

4.5 Generated magnetic field B_s in a rotating superconducting slab

Using equation 3.21, we then calculate values of generated magnetic fields, B_s for different values of slab thickness d , ultrasound angular velocity ω , ultrasound amplitude U_0 and rotational angular velocity Ω as shown in tables 4.6, 4.7 and 4.8.

Table 4.6: Calculated values of generated magnetic field B_s , for different values of ultrasound angular velocity ω , and rotational angular velocity Ω of the superconducting slab of varying slab thickness, d . The ultrasound amplitude is constant, $U_0 = 0.15$ nm.

d (m) $\times 10^{-6}$	ω_s (Hz) $\times 10^9$	Ω (s^{-1}) $\times 10^6$	B_s (T) $\times 10^3$
0.25	6.60	6.22	42.40
0.40	4.13	2.43	16.60
0.50	3.30	1.56	10.60
0.60	2.75	1.08	7.40
0.75	2.20	0.69	4.71
0.90	1.83	0.48	3.28
1.00	1.65	0.39	2.70
1.25	1.32	0.25	1.71
1.50	1.10	0.17	1.16
1.75	0.94	0.13	0.89

A graph of generated magnetic field, B against the rotational angular velocity, Ω of the superconductor is then plotted ultrasound amplitude is constant, $U_o = 0.15 \text{ nm}$.

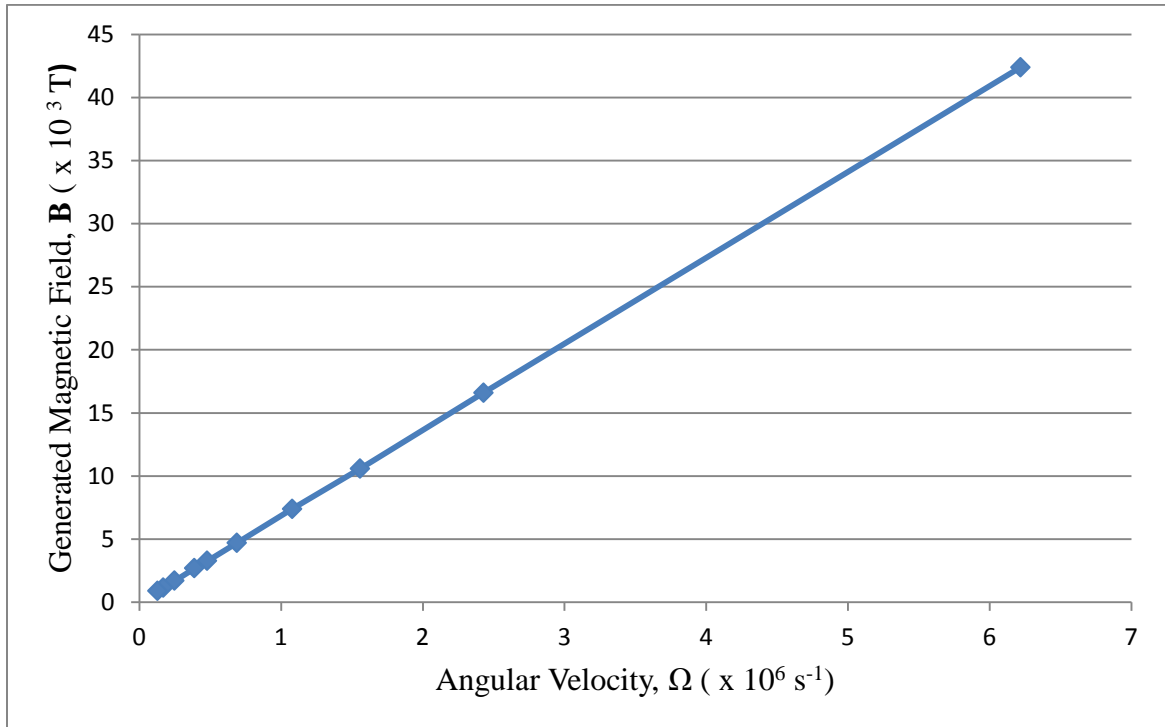


Figure 4.7: Indicates a positive linear relationship between the angular velocity, Ω of the rotating superconducting slab and the generated magnetic field, B_s when the ultrasound amplitude is 0.15nm.

The equation of this straight line is:

$$B_s = 6.82 \times 10^{-3} \Omega$$

4.9

Table 4.7: Calculated values of generated magnetic field B_s , for different values of ultrasound angular velocity ω , and angular velocity Ω of rotation of the superconducting slab of varying slab thickness, d . The ultrasound amplitude is constant, $U_0 = 0.23$ nm.

d (m) $\times 10^{-6}$	ω_s (Hz) $\times 10^9$	Ω (s^{-1}) $\times 10^6$	B_s (T) $\times 10^3$
0.25	6.60	9.54	65.10
0.40	4.13	3.73	25.50
0.50	3.30	2.38	16.20
0.60	2.75	1.66	11.30
0.75	2.20	1.06	7.23
0.90	1.83	0.73	4.98
1.00	1.65	0.60	4.09
1.25	1.32	0.38	2.59
1.50	1.10	0.26	1.77
1.75	0.94	0.19	1.30

A graph of generated magnetic field, B against the rotational angular velocity, Ω of the superconductor is then plotted ultrasound amplitude is constant, $U_o = 0.23 \text{ nm}$.

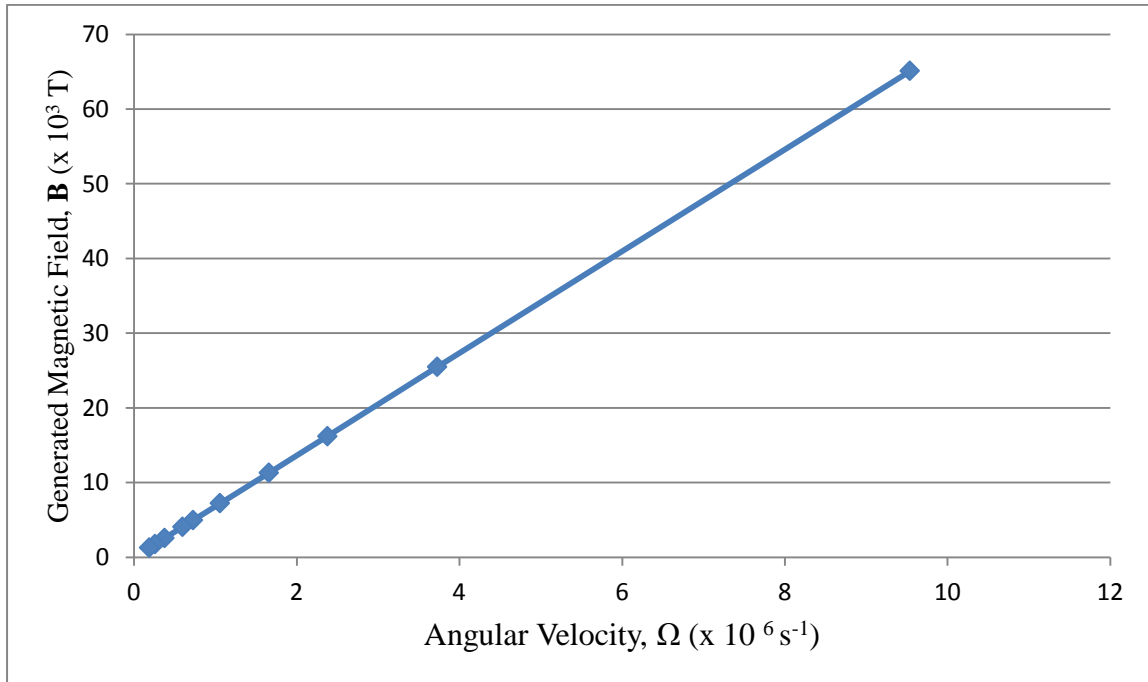


Figure 4.8: Indicates a positive linear relationship between the angular velocity, Ω of the rotating superconducting slab and the generated magnetic field, B_s when the ultrasound amplitude is 0.23 nm .

The equation of this straight line is:

$$B_s = 6.82 \times 10^{-3} \Omega$$

4.10

Table 4.8: Calculated values of generated magnetic field B_s , for different values of ultrasound angular velocity ω , and rotational angular velocity Ω of the superconducting slab of varying slab thickness, d . The ultrasound amplitude is constant, $U_0 = 0.40$ nm.

d (m) $\times 10^{-6}$	ω_s (Hz) $\times 10^9$	Ω (s^{-1}) $\times 10^6$	B_s (T) $\times 10^3$
0.25	6.60	16.59	113.19
0.40	4.13	6.49	44.28
0.50	3.30	4.15	28.32
0.60	2.75	2.88	19.65
0.75	2.20	1.84	12.55
0.90	1.83	1.28	8.73
1.00	1.65	1.04	7.10
1.25	1.32	0.66	4.50
1.50	1.10	0.46	3.14
1.75	0.94	0.34	2.32

A graph of generated magnetic field, B against the rotational angular velocity, Ω of the superconductor is then plotted ultrasound amplitude is constant, $U_0 = 0.40$ nm.

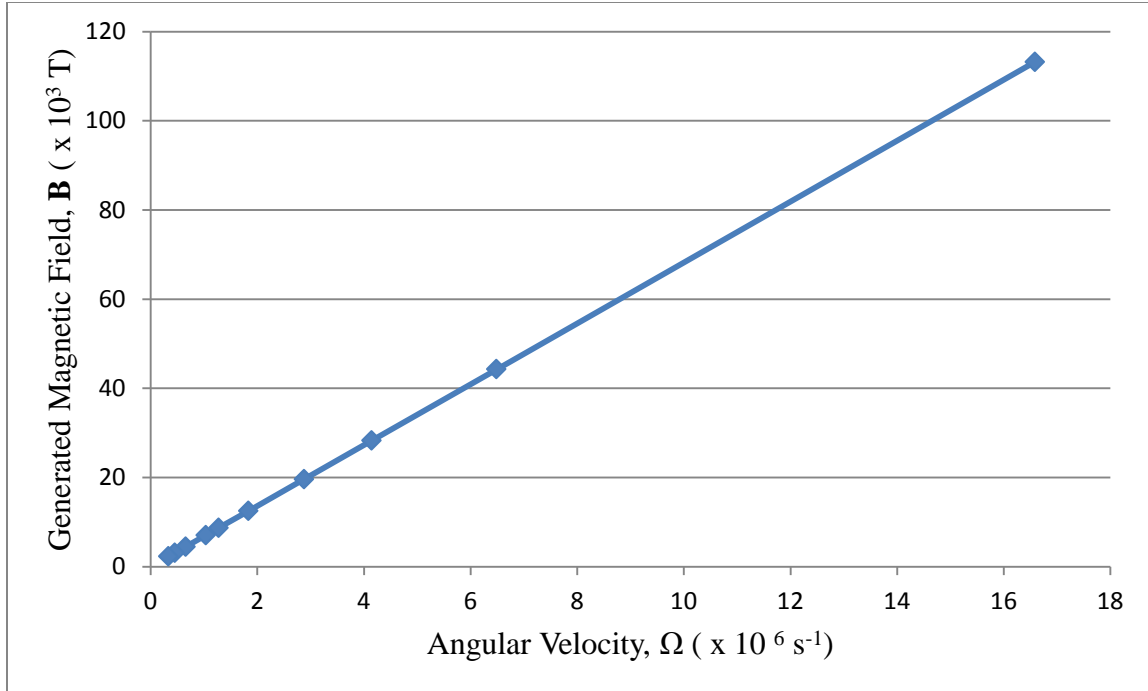


Figure 4.9: Indicates a positive linear relationship between the angular velocity, Ω of the rotating superconducting slab and the generated magnetic field, B_s when the ultrasound amplitude is 0.40nm.

The equation of this straight line is:

$$\mathbf{B}_s = 6.82 \times 10^{-3} \Omega \quad 4.10$$

Different values of ultrasound amplitude U_0 yield different values of magnetic fields, \mathbf{B}_s as shown in tables 4.6, 4.7 and 4.8 in which the ultrasound amplitude U_0 is varied from 0.15 nm to 0.40 nm. These tables 4.6, 4.7 and 4.8 show that to produce a certain magnetic field \mathbf{B}_s lower than some higher value, both the angular velocities Ω (rotational angular velocity of the superconducting cylinder and ω (angular velocity of ultrasound) have to be decreased. This means that as the rotational angular velocity, Ω and ω are lowered, the value of \mathbf{B}_s decreases for an increasing slab thickness, d .

It should also be noted from the calculations in tables 4.6, 4.7 and 4.8 that increasing the ultrasound amplitude U_0 increases the rotational angular velocity Ω of the superconducting slab and magnetic field B_s generated for constant values of the slab thickness d and ultrasound angular velocity ω .

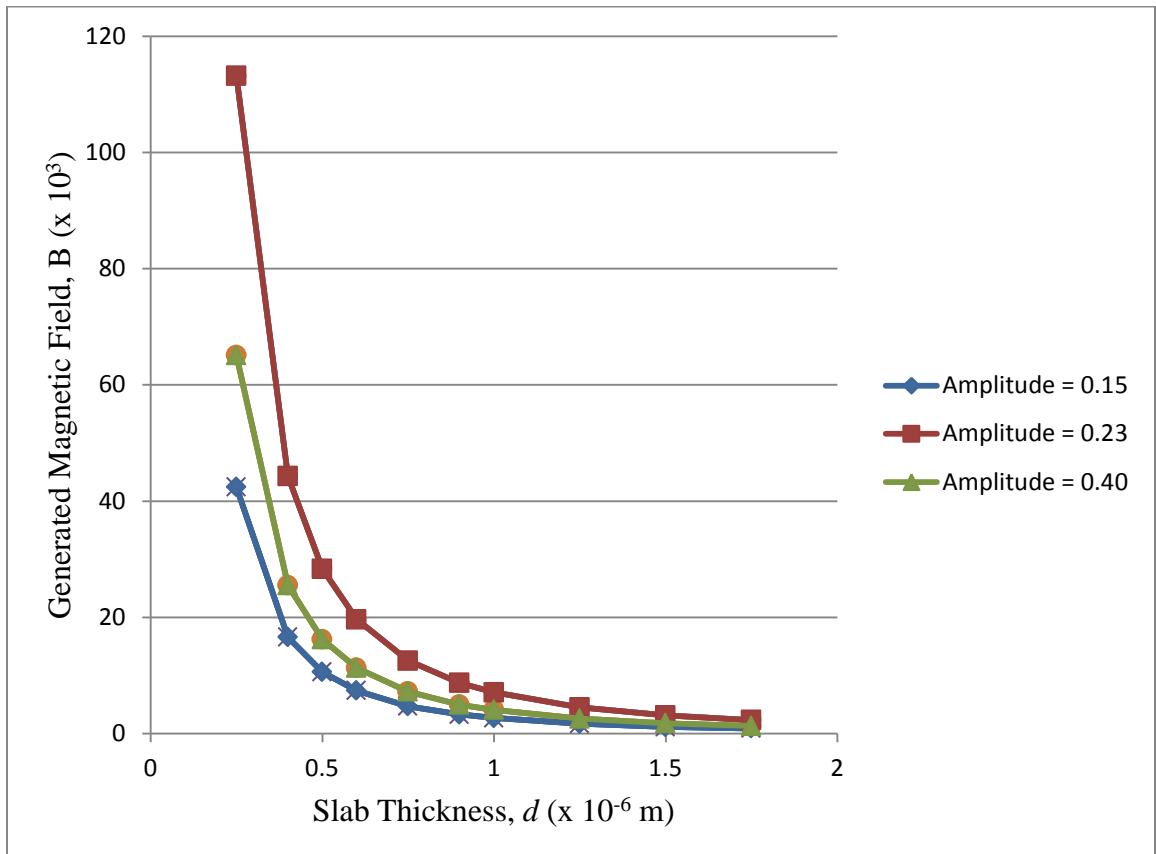


Figure 4.10: Relationship between the generated magnetic field B , and the slab thickness d , of the superconducting cylinder for different values of ultrasound amplitude, $U_0 = 0.15, 0.23$ and 0.40 nm.

From figure 4.10 it is evident that rotational angular velocity Ω of the superconducting cylinder and the generated magnetic fields B_s are both directly proportional to the ultrasound amplitude U_0 for decreasing values of rotating slab

thickness d and increasing values of ultrasound angular velocity, ω_s . It also shows the exponential nature of the curves that are much steeper for slab thickness, d of values between 0.2×10^{-6} and 0.4×10^{-6} m and generated magnetic field \mathbf{B}_s of values above 20 kT. Increasing the slab thickness beyond $1\mu\text{m}$ does not lead to substantial decrease in the generated magnetic field, \mathbf{B}_s .

Equations 4.9, 4.10 and 4.11 are the same which indicates that, irrespective of the ultrasound amplitude U_o , the generated magnetic field \mathbf{B}_s varies directly as the rotational angular velocity Ω of the superconducting slab for decreasing values of the slab thickness, d and decreasing values of the ultrasound angular velocity, ω_s . The constant of proportionality is 6.82×10^{-3} .

Using equation 3.21, a number of values of generated magnetic field \mathbf{B}_s (T) $\approx H_{c1}$ have been obtained for different values of ultrasound amplitude U_o (0.15nm, 0.23nm and 0.40 nm), rotating slab thickness d (ranging from $0.25 \mu\text{m}$ to $1.75 \mu\text{m}$), calculated rotational angular velocity Ω (ranging from 0.13×10^6 to $16.59 \times 10^6 \text{ s}^{-1}$) of the superconducting cylinder and ultrasound angular velocity ω_s (ranging from 0.94×10^9 to 6.60×10^9 Hz) for the nucleation of superconducting vortices. Equation 4.9 is one major result obtained. It defines the relationship between the generated magnetic field \mathbf{B}_s and the rotational angular velocity Ω of the superconducting cylinder. This equation gives a constant of proportionality of 6.82×10^{-3} irrespective of the values of U_o, Ω, d and ω_s .

CHAPTER FIVE

CONCLUSIONS AND RECOMMENDATIONS

5.1 Conclusions

The calculations in chapter 4 have enabled us to theoretically generate values of fictitious magnetic fields \mathbf{B}_s , of the order 10^3 T that exceed H_{c1} (which is around 0.2 T). These \mathbf{B}_s values range from 0.89×10^3 T to 113.19×10^3 T (from tables 4.6, 4.7 and 4.8). This has been possible with high frequency ultrasound (in the gigahertz frequency range) ranging from 0.94×10^9 Hz to 6.60×10^9 Hz as calculated from table 4.1.

As Ω (the angular velocity of the rotating superconducting cylinder) changes its sign every half a period of the sound, vortices are periodically attracted and repelled by the standing acoustic wave. Ultrasound of velocity 3,300 m/s is required to cause nucleation. Periodic entering and expulsion of vortices should result in the elevated attenuation of the ultrasound and in the ac voltage across the slab at the sound frequency.

In conclusion, we have demonstrated that nucleation of a vortex in a superconductor can be assisted by ultrasound of amplitude ranging from 0.15 to 0.40 nm that have been calculated using equation 4.3. In the presence of a standing sound wave, vortices will periodically enter and exit the superconductor. The required amplitude and frequency of ultrasound are within experimental reach.

5.2 Recommendations for Future Research

There are two distinct forms of superconductivity. The conventional superconductivity that is explained by the BCS theory. Such superconductors are mostly metals and doped semiconductors. The other form of superconductivity is called the high T_c superconductivity. Such superconductors are mostly poor conductors and oxides. There are others that are called layered high T_c superconductors.

Different types of superconducting cylinders can be made and rotated to develop magnetic moment. The quantum of magnetic flux and the penetration depth of the field can be measured. Appropriate theories can be developed and experimental and theoretical results compared.

REFERENCES

1. Mourachkine, A. (2004). *Room-temperature superconductivity*. Cambridge Int Science Publishing.
2. Kresin, V. Z., & Wolf, S. A. (1990). Major normal and superconducting parameters of high-T_c oxides. *Physical Review B*, 41(7), 4278.
3. Bardeen, J., Cooper, L. N., & Schrieffer, J. R. (1957). Theory of superconductivity. *Physical Review*, 108(5), 1175.
4. Wesche, R. (2007). *High-temperature superconductors* (pp. 1193-1218). Springer US.
5. Albert, J., & Chudnovsky, E. M. (2008). Nucleation of superconducting vortices by exciting acoustic standing waves in a type-II superconductor. *Physical Review B*, 77(9), 092506.
6. Barnett, S. J., & Kenny, G. S. (1952). Gyromagnetic Ratios of Iron, Cobalt, and Many Binary Alloys of Iron, Cobalt, and Nickel. *Physical Review*, 87(5), 723.
7. Meissner, W., & Ochsenfeld, R. (1933). "Naturwiss. 21, 787 "H. London and F. London." (*London*) A. Vol. 149. 1935.
8. Onnes, H.K. (1911), Commun. Phys. Lab. Univ. Leiden 12, 120.
9. Khanna, K.M. (2008). Superconductivity. *Moi University Inaugural lecture 3 series No. 1*
10. Johnston, H. (2009). *Type-1.5 Superconductor shows its stripes*. *Physics World* (Institute of Physics).
11. Narlikar, A. V., & Ekbote, S. N. (1983). *Superconductivity and superconducting materials*. New Delhi: South Asian Publishers.

12. Poole, , Horacio A., Richard J. C. (2010): *Superconductivity* - Academic Press
13. P Jr, P. C. (2000). Handbook of Superconductivity.
14. <http://www.wordiq.com/definition/Superconductivity>
15. London, F. (1950). Superfluids, volume I.
16. de Lima Jr, M. M., & Santos, P. V. (2005). Modulation of photonic structures by surface acoustic waves. *Reports on progress in physics*, 68(7), 1639.
17. Abrikosov, A. A. (1957). Zh. É ksp. Teor. Fiz. 32, 1442 1957 Sov. Phys. *JETP*, 5, 1174.
18. Chapman, S. J. (1995). A mean-field model of superconducting vortices in three dimensions. *SIAM Journal on Applied Mathematics*, 55(5), 1259-1274.
19. Bean, C. P., & Livingston, J. D. (1964). Surface barrier in type-II superconductors. *Physical Review Letters*, 12(1), 14.
20. Boato, G., Gallinaro, G., & Rizzuto, C. (1965). Direct evidence for quantized flux threads in type-II superconductors. *Solid State Communications*, 3(8), 173-176.
21. Chapman, S. J. (1995). Superheating field of type II superconductors. *SIAM Journal on Applied Mathematics*, 55(5), 1233-1258.
22. Saffman, P. G. (1992). *Vortex dynamics*. Cambridge university press.
23. García-Ripoll, J. J., & Pérez-García, V. M. (2001). Vortex nucleation and hysteresis phenomena in rotating Bose-Einstein condensates. *Physical Review A*, 63(4), 041603.
24. Madison, K. W., Chevy, F., Wohlleben, W., & Dalibard, J. (2000). Vortex formation in a stirred Bose-Einstein condensate. *Physical Review Letters*, 84(5), 806.

25. Teller, E. (1962). On the stability of molecules in the Thomas-Fermi theory. *Reviews of Modern Physics*, 34(4), 627.
26. J. García-Ripoll, J. J., & Pérez-García, V. M. (2001). Vortex nucleation and hysteresis phenomena in rotating Bose-Einstein condensates. *Physical Review A*, 63(4), 041603.
27. Butts, D. A., & Rokhsar, D. S. (1999). Predicted signatures of rotating Bose-Einstein condensates. *Nature*, 397(6717), 327-329.
28. Wigner, E. (1934). On the interaction of electrons in metals. *Physical Review*, 46(11), 1002.
29. Vorov, O. K., Van Isacker, P., Hussein, M. S., & Bartschat, K. (2005). Nucleation and growth of vortices in a rotating Bose-Einstein condensate. *Physical review letters*, 95(23), 230406.
30. Williams, R. A., Al-Assam, S., & Foot, C. J. (2010). Observation of vortex nucleation in a rotating two-dimensional lattice of Bose-Einstein condensates. *Physical review letters*, 104(5), 050404.